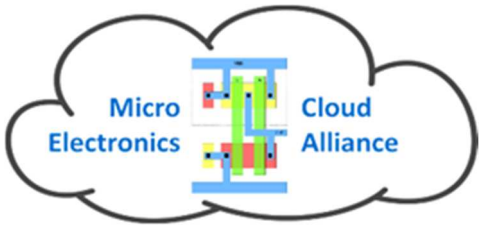

Superconductive materials

Thin Films in Energy Saving Technologies

The project has been funded with the support of the European Commission

Contents

2.3. Analysis of composition: EDX/EPMA, XPS.

2.4. Analysis of microstructure: SEM, AFM.

3. Superconductive wires.

3.1. Superconductivity phenomenon, history, materials.

3.2. 1st and 2nd generation (G) of high temperature superconductive (HTS) wires.

3.2.a. Comparison of superconductive materials and concepts used in 1G and 2G-HTS-wires.

3.2.b. Overview of fabrication technologies for 2G-HTSW.

3.3. Application of HTS-Wires.

3.3.a. Awaited profit, cooling systems, very future technologies.

3.3.a. Cables, FLCs (fault-current limiters).

3.3.b. Generators, motors.

3.3.c. Energy reserves, Inductive heaters.

4. Photovoltaic.

4.1. Basics and overview of existing technologies.

4.2. Main thin film technologies.

4.2.a. *a*-Si/□*c*-Si tandem cells, structure, production.

4.2.b. CIGS based cells, structure, production.

4.2.c. TCO (transparent conductive oxides) in solar cells.

4.3. Characterization of efficiency (sun simulator, I-V curves, mapping).

5. New concepts and materials in energy saving technologies.

5.1. New concepts and materials in Photovoltaics (PV).

5.1.a. Hybrid organometallic halide perovskite absorber based PV.

5.1.b. Dye-sensitized solar cells, organic PV.

5.1.c. New concepts of batteries.

5.2. Oxide electronics: advantages, state-of-the-art.

Introduction

A thin film is a layer of material ranging from fractions of a nanometer (monolayer) to several micrometers in thickness. Electronic semiconductor devices and optical coatings are the main applications benefiting from thin-film construction.

Table 1. Thin film applications. *[Smith 1995]*

Thin-film property category	Typical applications
Optical	Reflective/antireflective coatings Interference filters Decoration (color, luster) Memory discs (CDs) Waveguides
Electrical	Insulation Conduction Semiconductor devices Piezoelectric drivers
Magnetic	Memory discs
Chemical	Barriers to diffusion or alloying Protection against oxidation or corrosion Gas/liquid sensors
Mechanical	Tribological (wear-resistant) coatings Hardness Adhesion Micromechanics
Thermal	Barrier layers Heat sinks

A familiar application of thin films is the household mirror, which typically has a thin metal coating on the back of a sheet of glass to form a reflective interface. The process of silvering was once commonly used to produce mirrors. A very-thin-film coating (less than about 50 nanometers thick) is used to produce two-way mirrors.

The performance of optical coatings (e.g., antireflective, or AR, coatings) are typically enhanced when the thin-film coating consists of multiple layers having varying thicknesses and refractive indices. Similarly, a periodic structure of alternating thin films of different materials may collectively form a so-called superlattice which exploits the phenomenon of quantum confinement by restricting electronic phenomena to two-dimensions.

Work is being done with ferromagnetic and ferroelectric thin films for use as computer memory. It is also being applied to pharmaceuticals, via thin-film drug delivery. Thin-films are used to produce thin-film batteries. Thin films are also used in dye-sensitized solar cells.

Ceramic thin films are in wide use. The relatively high hardness and inertness of ceramic materials make this type of thin coating of interest for protection of substrate materials against corrosion, oxidation and wear. In particular, the use of such coatings on cutting tools can extend the life of these items by several orders of magnitude.

Research is being done on a new class of thin-film inorganic oxide materials, called amorphous heavy-metal cation multicomponent oxides, which could be used to make transparent transistors that are inexpensive, stable, and environmentally benign.

Thin-film technologies are also being developed as a means of substantially reducing the cost of photovoltaic (PV) systems. The rationale for this is that thin-film modules are cheaper to manufacture owing to their reduced material costs, energy costs, handling costs and capital costs. This is especially represented in the use of printed electronics (roll-to-roll) processes. Thin films belong to the second and third photovoltaic cell generations.

Thin-film printing technology is being used to apply solid-state lithium polymers to a variety of substrates to create unique batteries for specialized applications. Thin-film batteries can be deposited directly onto chips or chip packages in any shape or size. Flexible batteries can be made by printing onto plastic, thin metal foil, or paper.

Table 2. Overview on material demands

	Material demands
Index	■ **Heat treatable high index** (crucial for glazing applications) ■ **Precise deposition** of smooth multilayers (for AR & optical filters)
Durable	■ Low haze, **mechanical stable**, stable functional properties
Semiconductor	■ TFT: **High mobility, high resistivity** ■ PV: Band alignment
Contact layers	■ Tailored optical window & low absorption (e. g. **high mobility TCOs**) ■ Band alignment
Barrier	■ On glass: Sodium diffusion barrier ■ Ultra barriers for organic electronics: Coating defect compensating mechanisms

1. Overview of the film fabrication techniques

The act of applying a thin film to a surface is thin-film deposition – any technique for depositing a thin film of material onto a substrate or onto previously deposited layers. "Thin" is a relative term, but most deposition techniques control layer thickness within a few tens of nanometres. Molecular beam epitaxy allows a single layer of atoms to be deposited at a time. It is useful in the manufacture of optics (for reflective, anti-reflective coatings or self-cleaning glass, for instance), electronics (layers of insulators, semiconductors, and conductors form integrated circuits), packaging (i.e., aluminium-coated PET film). Deposition techniques fall into two broad categories, depending on whether the process is primarily chemical or physical.

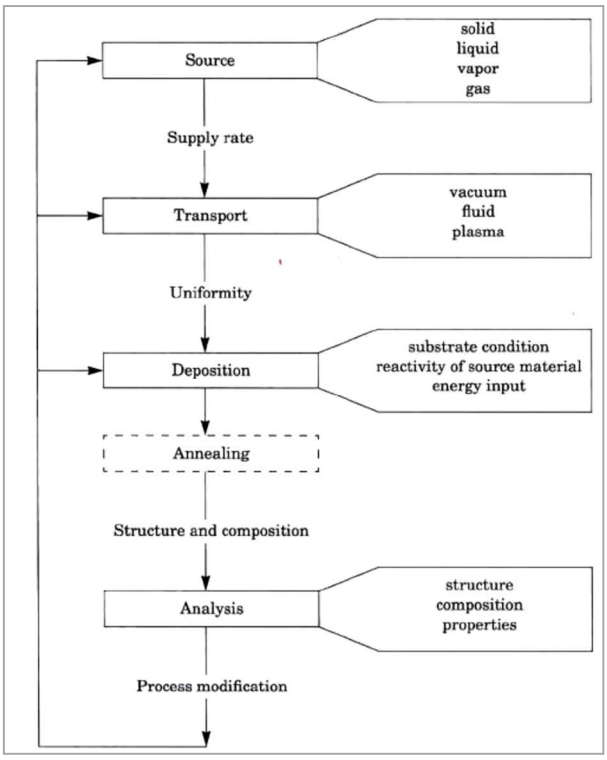

Fig. 1. Thin film process steps. In all steps, process monitoring is valuable, and contamination is a concern *[Smith 1995]*.

Chemical deposition

Here, a fluid precursor undergoes a chemical change at a solid surface, leaving a solid layer. Since the fluid surrounds the solid object, deposition happens on every surface, with little regard to direction; thin films from chemical deposition techniques tend to be conformal, rather than directional.

Chemical deposition is further categorized by the phase of the precursor:

- **Plating** relies on liquid precursors, often a solution of water with a salt of the metal to be deposited. Some plating processes are driven entirely by reagents in the solution (usually for noble metals), but by far the most commercially important process is electroplating. It was not commonly used in semiconductor processing for many years, but has seen a resurgence with more widespread use of chemical-mechanical polishing techniques.
- **Chemical solution deposition** (CSD) or Chemical bath deposition (CBD) uses a liquid precursor, usually a solution of organometallic powders dissolved in an organic solvent. This is a relatively inexpensive, simple thin film process that is able to produce stoichiometrically accurate crystalline phases. This technique is also known as the sol-gel method because the 'sol' (or solution) gradually evolves towards the formation of a gel-like diphasic system.
- **Spin coating** or spin casting, uses a liquid precursor, or sol-gel precursor deposited onto a smooth, flat substrate which is subsequently spun at a high velocity to centrifugally spread the solution over the substrate. The speed at which the solution is spun and the viscosity of the sol determine the ultimate thickness of the deposited film. Repeated depositions can be carried out to increase the thickness of films as desired. Thermal

treatment is often carried out in order to crystallize the amorphous spin coated film. Such crystalline films can exhibit certain preferred orientations after crystallization on single crystal substrates.

- **Chemical vapor deposition (CVD)** generally uses a gas-phase precursor, often a halide or hydride of the element to be deposited. In the case of MOCVD, an organometallic gas is used. Commercial techniques often use very low pressures of precursor gas.
- **Plasma enhanced CVD (PECVD)** uses an ionized vapor, or plasma, as a precursor. Unlike the soot example above, commercial PECVD relies on electromagnetic means (electric current, microwave excitation), rather than a chemical reaction, to produce a plasma.
- **Atomic layer deposition (ALD)** uses gaseous precursor to deposit conformal thin films one layer at a time. The process is split up into two half reactions, run in sequence and repeated for each layer, in order to ensure total layer saturation before beginning the next layer. Therefore, one reactant is deposited first, and then the second reactant is deposited, during which a chemical reaction occurs on the substrate, forming the desired composition. As a result of the stepwise, the process is slower than CVD, however it can be run at low temperatures, unlike CVD.

Physical deposition

Physical deposition uses mechanical, electromechanical or thermodynamic means to produce a thin film of solid. Since most engineering materials are held together by relatively high energies, and chemical reactions are not used to store these energies, commercial physical deposition systems tend to require a low-pressure vapor environment to function properly; most can be classified as **physical vapor deposition (PVD)**. The material to be deposited is placed in an energetic, entropic environment, so that particles of material escape its surface. Facing this source is a cooler surface which draws energy from these particles as they arrive, allowing them to form a solid layer. The whole system is kept in a vacuum deposition chamber, to allow the particles to travel as freely as possible. Since particles tend to follow a straight path, films deposited by physical means are commonly directional, rather than conformal.

Examples of physical deposition include:

- A thermal **evaporator** uses an electric resistance heater to melt the material and raise its vapor pressure to a useful range. This is done in a high vacuum, both to allow the vapor to reach the substrate without reacting with or scattering against other gas-phase atoms in the chamber, and reduce the incorporation of impurities from the residual gas in the vacuum chamber. Obviously, only materials with a much higher vapor pressure than the heating element can be deposited without contamination of the film. Molecular beam epitaxy is a particularly sophisticated form of thermal evaporation. An electron beam evaporator fires a high-energy beam from an electron gun to boil a small spot of material; since the heating is not uniform, lower vapor pressure materials can be deposited. The beam is usually bent through an angle of 270° in order to ensure that the gun filament is not directly exposed to the evaporant flux. Typical deposition rates for electron beam evaporation range from 1 to 10 nanometres per second. In molecular

beam epitaxy (MBE), slow streams of an element can be directed at the substrate, so that material deposits one atomic layer at a time. Compounds such as gallium arsenide are usually deposited by repeatedly applying a layer of one element (i.e., gallium), then a layer of the other (i.e., arsenic), so that the process is chemical, as well as physical. The beam of material can be generated by either physical means (that is, by a furnace) or by a chemical reaction (chemical beam epitaxy).

- **Sputtering** relies on a plasma (usually a noble gas, such as argon) to knock material from a "target" a few atoms at a time. The target can be kept at a relatively low temperature, since the process is not one of evaporation, making this one of the most flexible deposition techniques. It is especially useful for compounds or mixtures, where different components would otherwise tend to evaporate at different rates. Note, sputtering's step coverage is more or less conformal.It is also widely used in the optical media. The manufacturing of all formats of CD, DVD, and BD are done with the help of this technique. It is a fast technique and also it provides a good thickness control. Presently, nitrogen and oxygen gases are also being used in sputtering.
- **Pulsed laser deposition** systems work by an ablation process. Pulses of focused laser light vaporize the surface of the target material and convert it to plasma; this plasma usually reverts to a gas before it reaches the substrate.
- **Cathodic arc deposition (arc-PVD)** which is a kind of ion beam deposition where an electrical arc is created that literally blasts ions from the cathode. The arc has an extremely high power density resulting in a high level of ionization (30–100%), multiply charged ions, neutral particles, clusters and macro-particles (droplets). If a reactive gas is introduced during the evaporation process, dissociation, ionization and excitation can occur during interaction with the ion flux and a compound film will be deposited.
- **Electrohydrodynamic deposition (electrospray deposition)** is a relatively new process of thin film deposition. The liquid to be deposited, either in the form of nano-particle solution or simply a solution, is fed to a small capillary nozzle (usually metallic) which is connected to a high voltage. The substrate on which the film has to be deposited is connected to ground. Through the influence of electric field, the liquid coming out of the nozzle takes a conical shape (Taylor cone) and at the apex of the cone a thin jet emanates which disintegrates into very fine and small positively charged droplets under the influence of Rayleigh charge limt. The droplets keep getting smaller and smaller and ultimately get deposited on the substrate as a uniform thin layer.

1.1. Vacuum technique

(Ultra) high vacuum evaporation

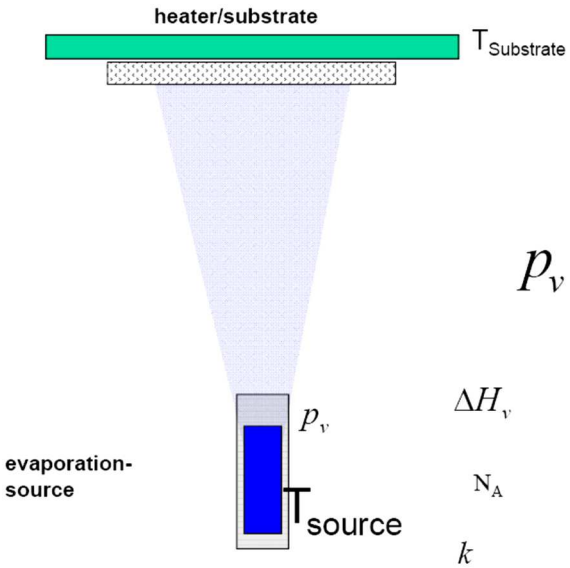

$$p_v = p_0 e^{-\Delta H_v / N_A kT}$$

ΔH_v	„latent heat“: enthalpy change per mole (in diesem Fall Verdampfungswärme)
N_A	Avogadro number
k	Boltzmann c $1{,}38^{-23}$ Ws/K, $8{,}62^{-5}$ eV/K
p_v	Pressure at the source

Fig. 2. Evaporation..

1.1.a. *Vacuum equipment*

1.1.b. *Gas dynamics, diffusion*

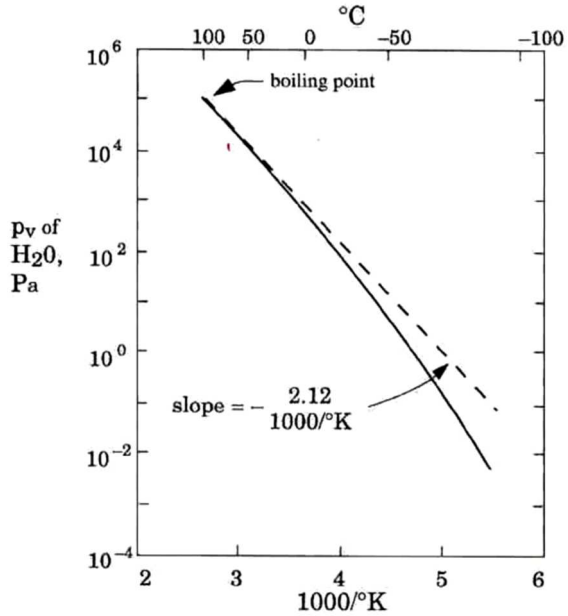

$$p_v = p_0 e^{-\Delta H_v / N_A kT}$$

Fig. 3. Vapor-pressure behavior of water.

1.1.c. *Energy of particles*

1.2. Plasma technique

Plasma is a collection of free charged particles moving in random directions, that is, on the average neutral.

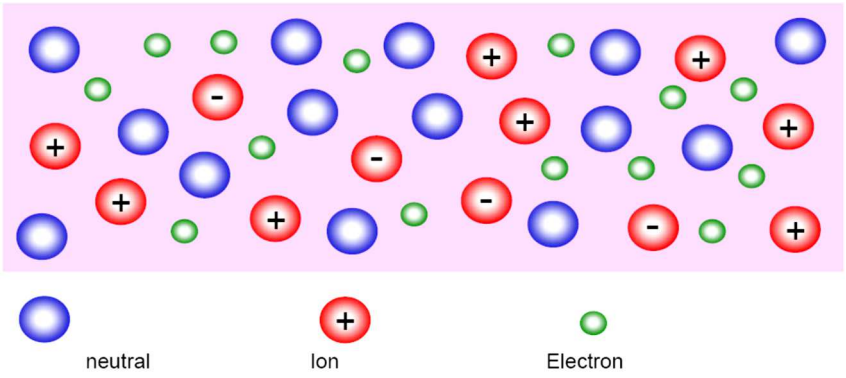

Fig. 4. Plasma..

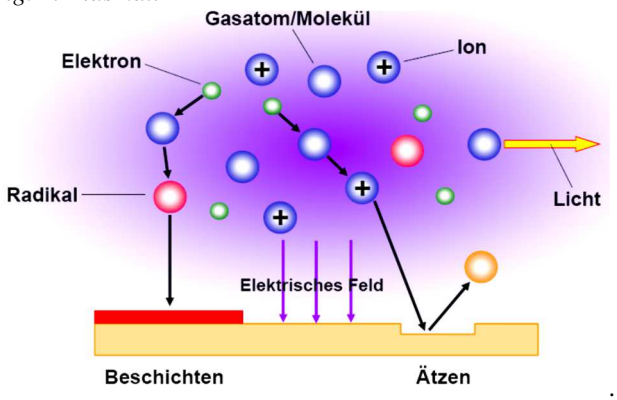

Fig. 5. Plasma as a tool for deposition and electro-etching.

1.2.a. *Equipment (generator, magnetron)*

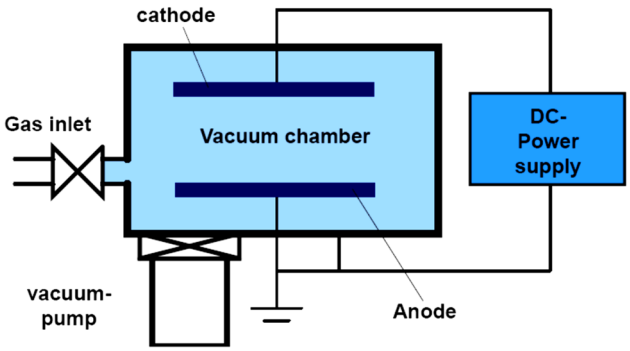

Fig. 6. Simple glow discharge reactor

1.2.b. *Plasma properties*

1.2.c. *Reactive and nonreactive sputtering process*

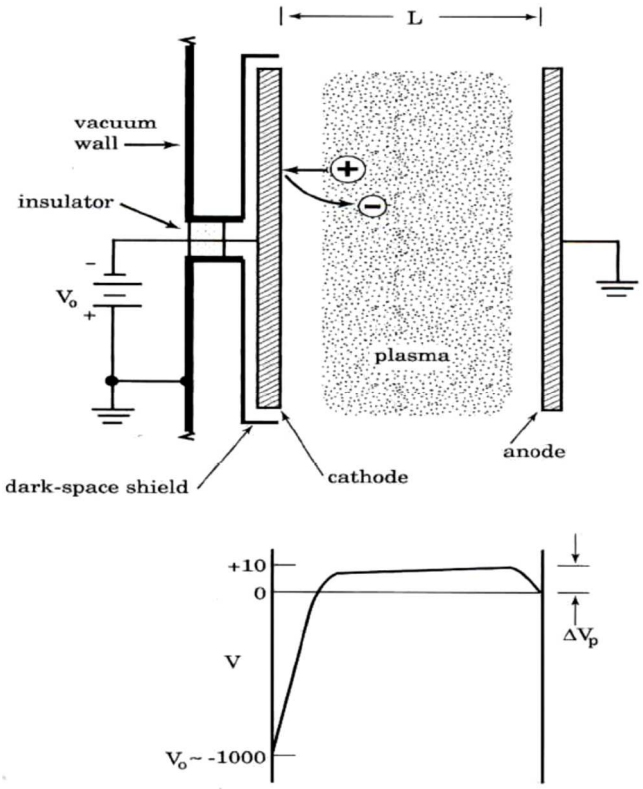

Fig. 7. Geometry and typical voltage profile of the parallel-plate dc glow discharge. [M.A. Liebermann and A. J.Lichtenberg, Principles of Plasma Discharges and Materials. Processing, John Wiley & Sons, New York 1994]

1.3. Film growth mechanisms: thermodynamics and kinetics of the film growth resulting in different microstructures

Deposition may be considered as six sequentional substeps:
The arriving atoms must

- Adsorption on the substrate
- Diffuse some distance before becoming absorbed in the film
- Incorporation involves reaction of the species with eachother and with the surface
- Nucleation: the initial aggregation of the film is called nucleation
- Structure development: As the film growth thicker it develops a structure or morphology which includes both (roughness) and crystallography (amorphous, fine crystalline, poly-crystalline, monocrystalline)
- Sometimes/finally, diffusional interactions occur within the bulk of the film, with the substrates or within interfaces of multilayers. Often post-treatments are applied.

Adsorption
An arriving molecule/atom feels an attraction from the surface molecules/atoms (van der Waals -force).
Physisorption/precursor state: the atom/molecule is mobile on the surface (involves only dipole interactions).
Chemisorption: involves the sharing of electrons – chemical bonds.

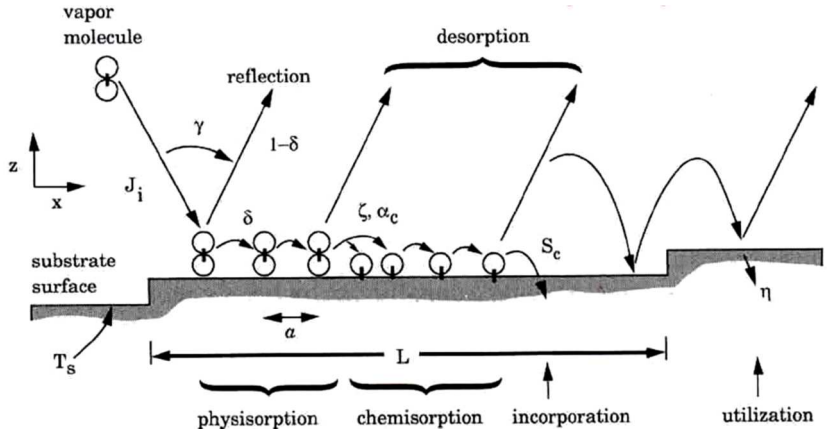

Fig. 8. Adsorption processes. Sc: sticking coefficient, fraction of the arriving vapour which becomes incorporated into the film.

Surface Diffusion - one of the most important determinants for film growth It allows the adsorbing species to find each others, to find the most active sides or find epitaxial sites.

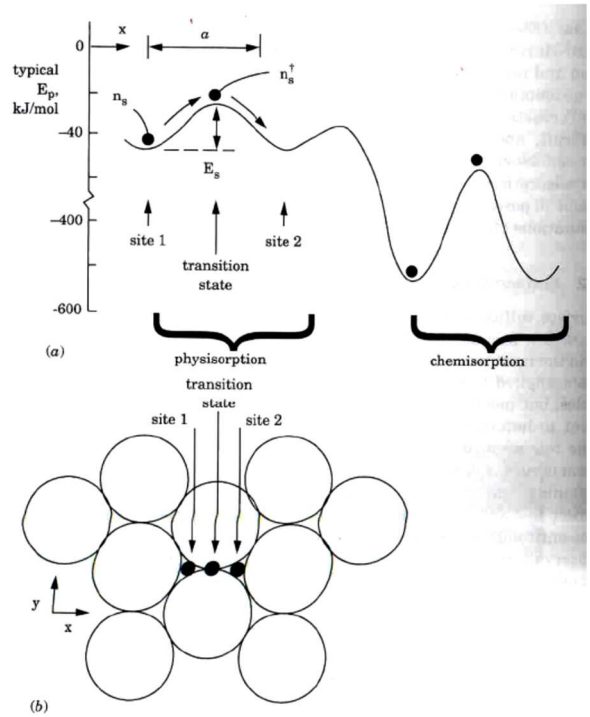

Fig. 9. Surface Diffusion: a) Potential energy vs. position x along the surface, and b) typical adsorption sites on a surface lattice.

Nucleation

a) The total surface energy of the wetted substrate is lower than for the bare one (strong bonding between film and substrate) – smooth growth.
b) If no strong bonds, spreading of the film across the substrate would always increase the total surface energy. This results in island growth (compare with waterdrop).
a) In specific situations the growth can change from layer by layer to island growth after one or two monolayers.

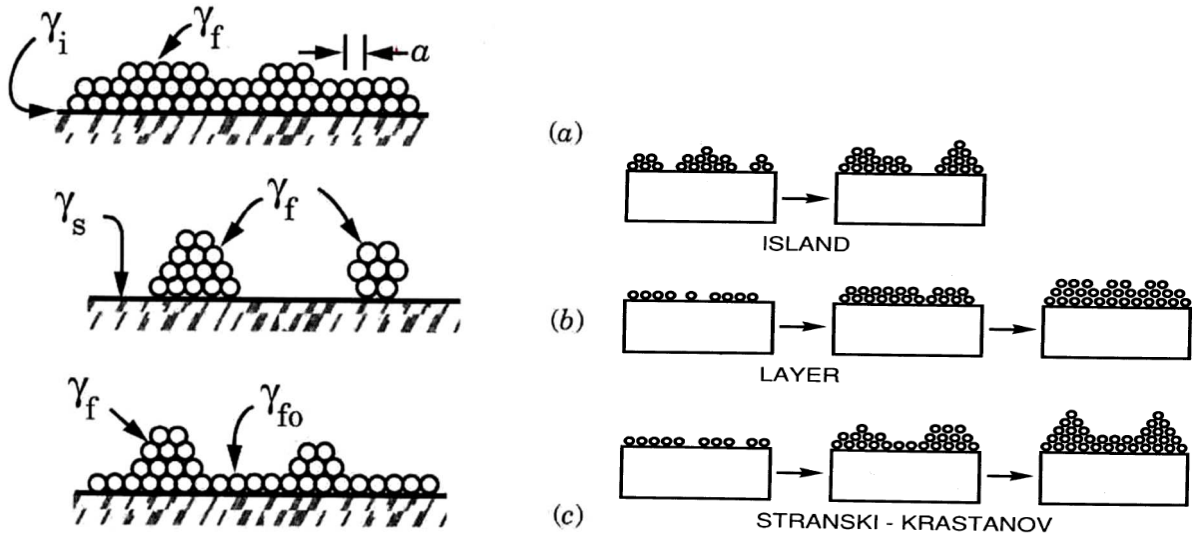

Fig. 10. Film growth modes: a) Frank-Wan der Merve (layer) b) Volmer-Weber (island), c) Stranski-Krastanov.

Structure development

- after coalescence of the surface nuclei to a continous film, the nucleation step of the film deposition is complete
- now, the development of the bulk film structure begins
- empirical model relates the growth to the relationship between TS: substrate temperature and TM: melting point of the film

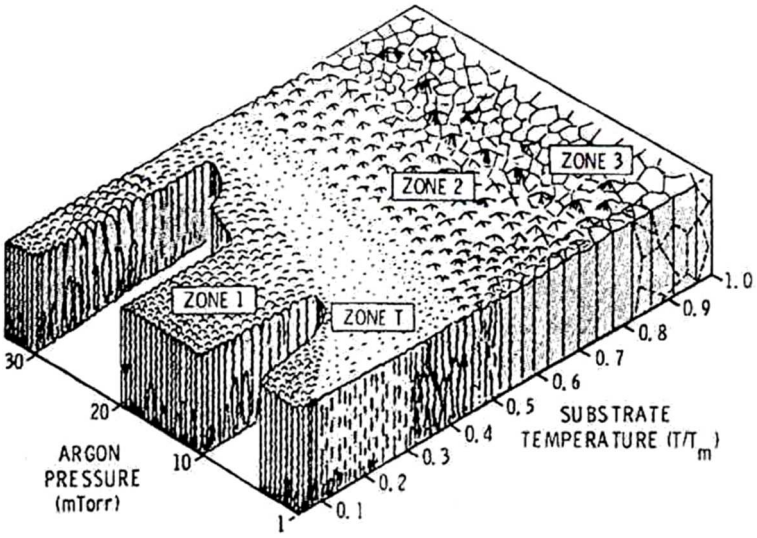

Fig. 11. Morphology of sputtered films. [Thornton, 1986].

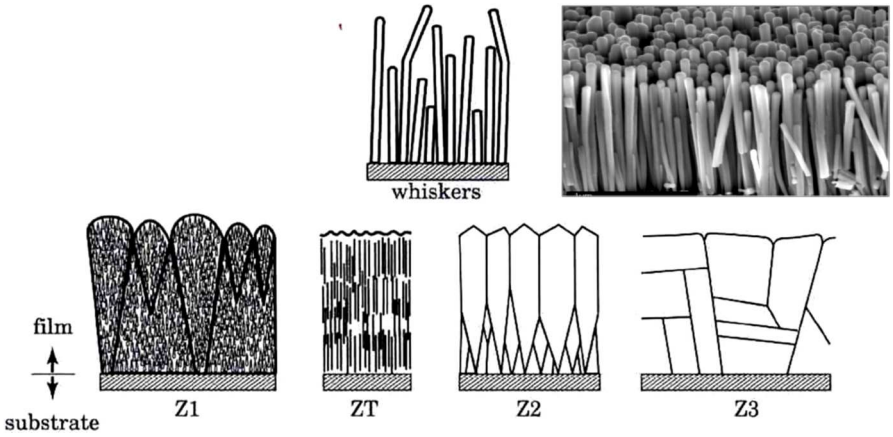

Fig. 12. Characteristics of the four basic structural zones and of whiskers, in cross section. The ration of the substrate T to film melting T (T_s/T_m) increases in the direction Z1→ ZT→ Z2 →Z3.

- Z1 occurs at Ts/Tm is low: surface diffusion is neglegible. The columns have poor crystallinity, many defects.
- ZT (transition zone) – similar to Z1 without voids and larger domains (usually associated with energy enhanced processes).
- Z2 occurs when Ts is high enough that surface diffusion become significant. It consists of tight grain boundaries.
- Z3 with further enhanced temperature (bulk annealing can take place) –the structure becomes isotropic The examples are typical for thin film growth, however, they do not appear in all types of materials.

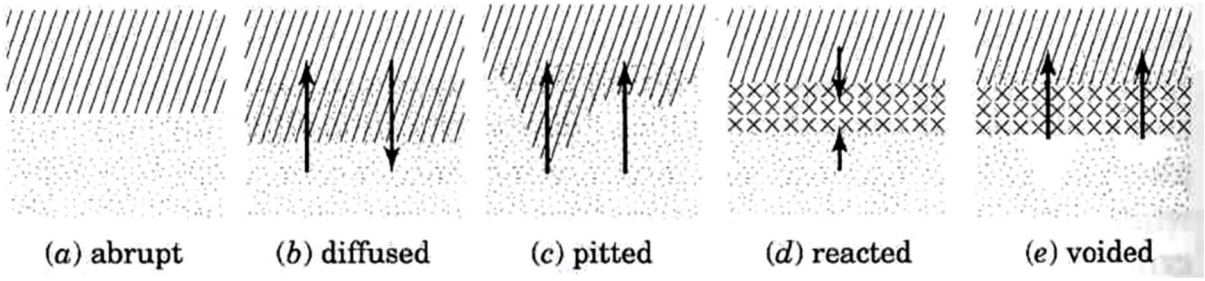

Fig. 13. Interfaces play an/the important role in thin film solar cells. This graph should just illustrate what can happen.

Surface energy consideration

The free-energy change accompanying the formation of an aggregate of mean dimention r is given by:

$$\Delta G = a_3 r^3 \Delta G_V + a_1 r^2 \gamma_{vf} + a_2 r^2 \gamma_{fs} - a_2 r^2 \gamma_{sv}$$

Chemical free-energy change per unit volume, ΔG_V, drives the condensation reaction, any level of gas oversaturation generates: ΔG_V <0, - > nucleation is possible.

Young' s equation:

$$\gamma_{sv} = \gamma_{fs} + \gamma_{vf} \cos\theta$$

for interfacial tensions (forces) .

Critical nucleus size (***r****) is the value of ***r*** when $d\,\Delta G / dr = 0$

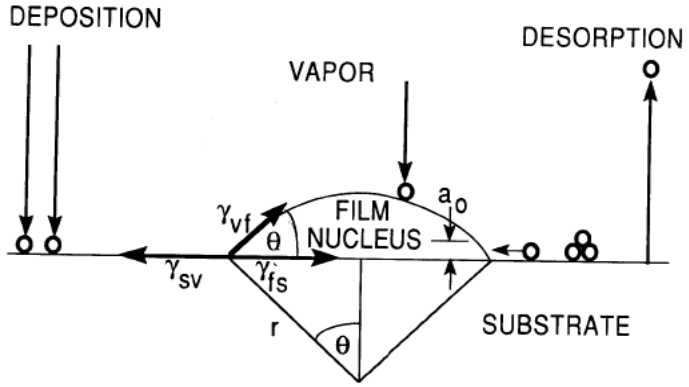

Fig.10. Schematic of basic atomistic processes on substrate surface during vapor deposition.

Nucleation kinetics

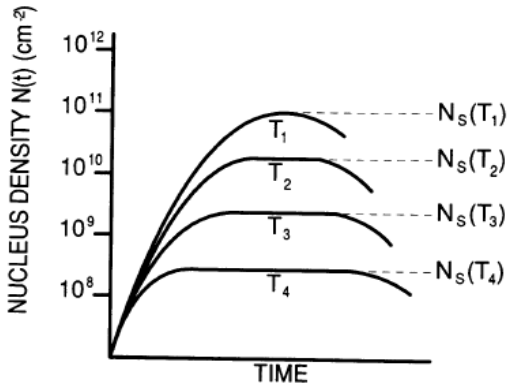

Fig.10. Schematic dependence of N(t) with time and substrate temperature: $T_4 > T_3 > T_2 > T_1$.

Nucleation rate: $$\dot{N} = 2\pi r^* a_0 \sin\theta \frac{PN_A}{\sqrt{2\pi MRT}} n_s \exp\frac{E_{des} - E_S - \Delta G^*}{kT}$$

E_s – activation energy for surface diffusion, E_{des} – activation energy of desorption, n_s – total nucleation site density.

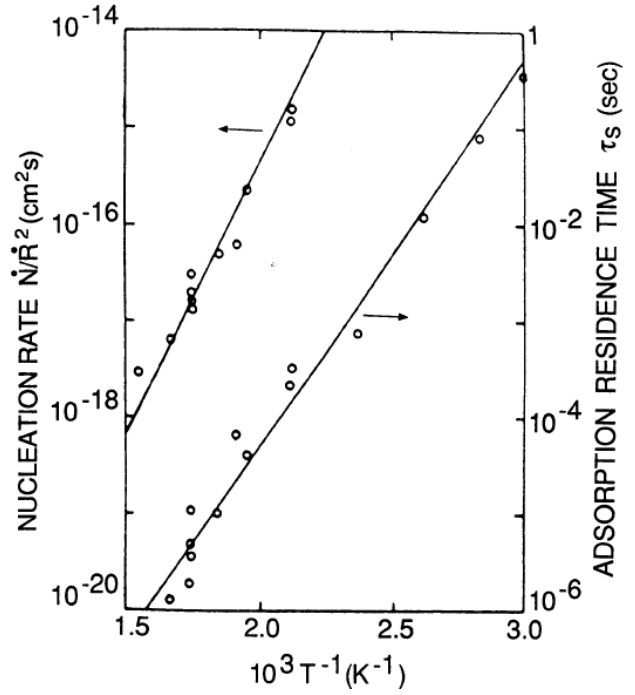

Fig.10. Plot of N/R^2 vs. 1IT (left) and tS vs. 1IT (right) for Au on KCl.

$$\tau_s = \frac{1}{\nu}\exp\frac{E_{\text{des}}}{kT}$$

ν – vibrational frequency, typically about 10^{12} s^{-1}

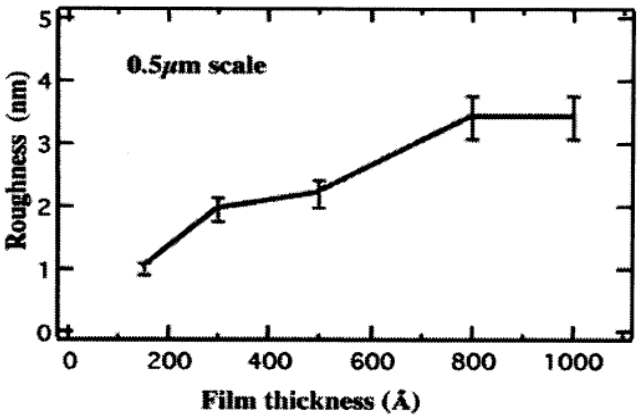

Fig.10. Evolution of the roughness as a function of the film thickness.

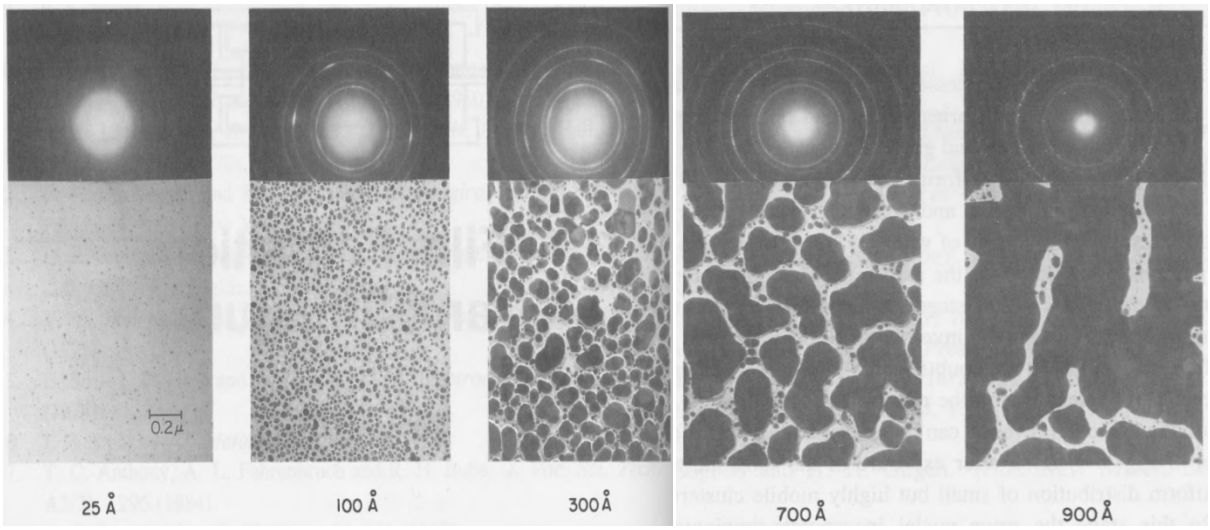

Fig.10. Particles' (2D) growth. Nucleation, growth and coalescence of Ag films on (111) NaCI substrates. Corresponding diffraction patterns are shown.

Coalescense

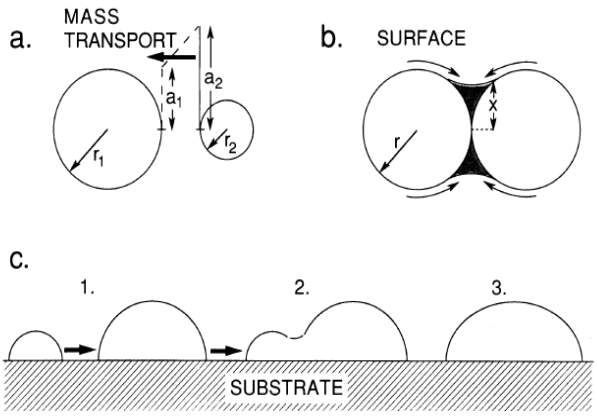

Fig.10. Coalescence of islands due to (a) Ostwald ripening, (b) sintering, (c) duster migration.

Surface diffusion is always larger than the lattice diffusion. At lower temperatures this difference is stronger.

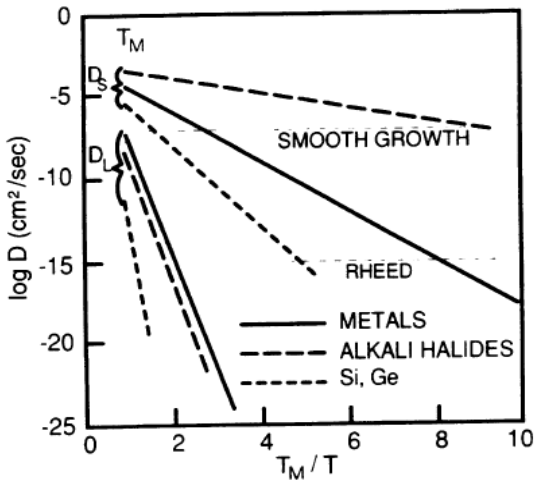

Fig.10. Lattice (D_L) and surface diffusivities (D_S) as a function of T_M/T for metals, semiconductors, and alkali halides.

„Zone theory“

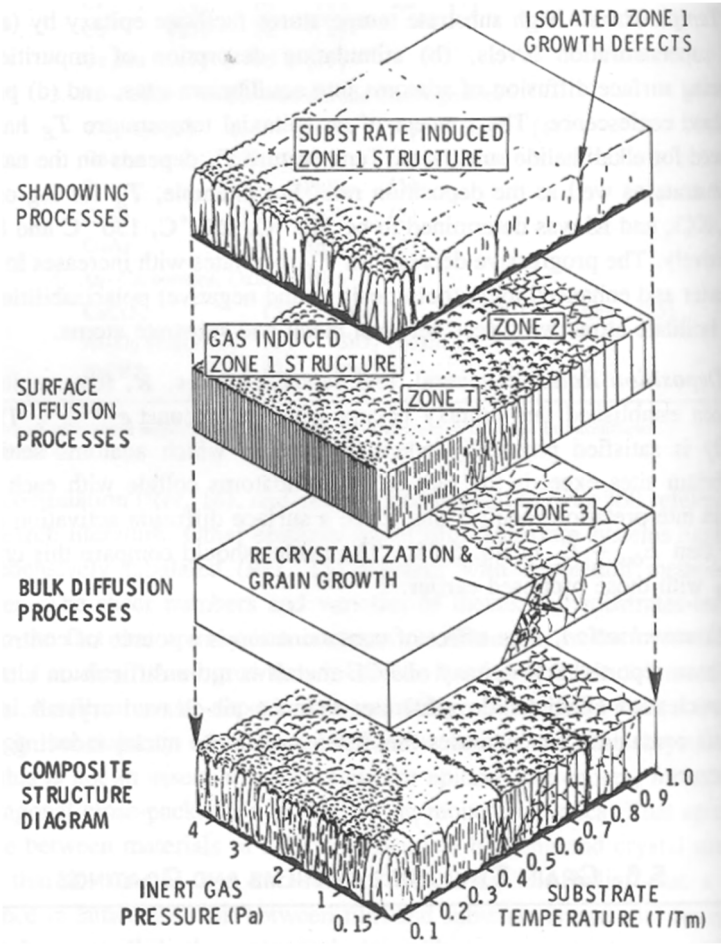

Fig.10. Schematic representation showing the Superposition of physical processes which establish structural zones. [J.V. Sanders, in “Chemisorption and Reactions on Metal Films”, J.R. Anderson (ed.), New York, Academic Press, vol. 1. 1971, 555 p].

Epitaxy phenomenon

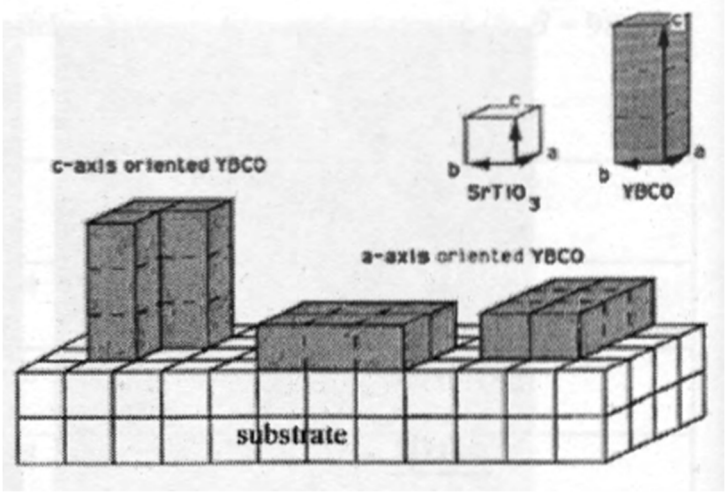

Fig.10. Epitaxy of [001] and [100] YBCO on (100) substrate.

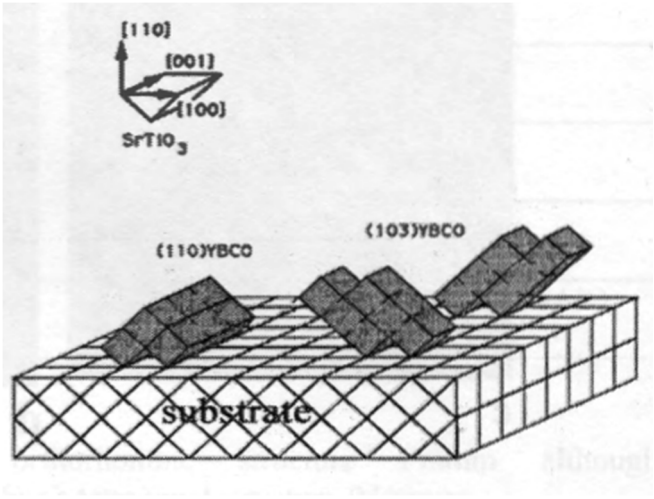

Fig.10. Epitaxy of [103] and [110] YBCO on (110) substrate.

1.4. *Overview of Plasma Deposition Methods*

1.4.a. *DC/MF/RF Magnetron Sputtering*

1.4.b. *Megatron, HIPIMS, other techniques*

1.5. CVD – Chemical vapor deposition

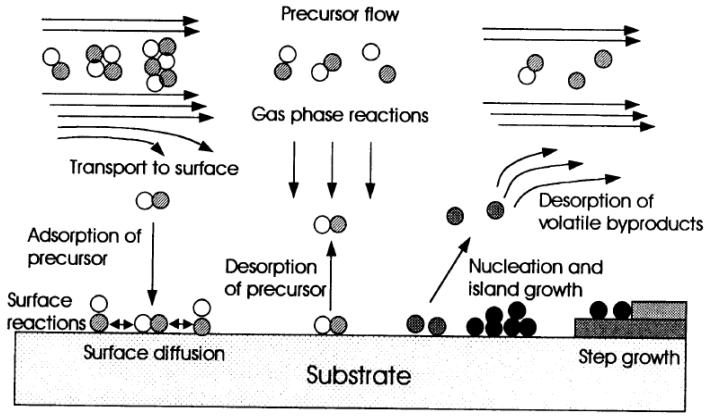

Fig. 11. Film growth from vapour. Fundamental processes active in the CVD process.

1.5.a. *CVD principles, theory*

1.5.b. *Hardware of CVD (evaporation systems, hot wall, cold wall reactors, R2R)*

1.5.c. *Examples of CVD processes, industrial use*

MOCVD (Metal Organic Chemical Vapour Deposition)

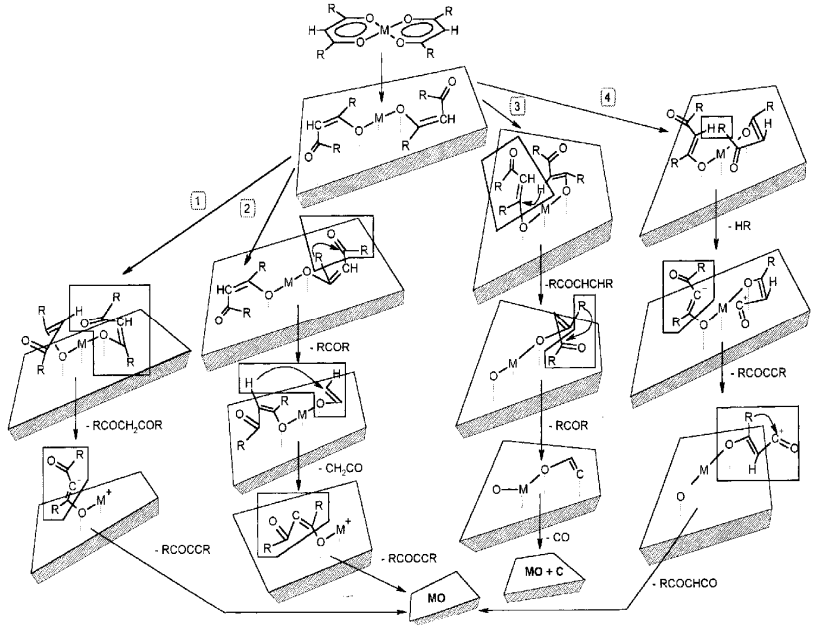

Fig.10. Chemical transformation of β-diketonate of metal in MOCVD process.

$$C_xH_yO_zM + O_2 \rightarrow x\ CO_2/CO + y/2\ H_2O + MO_n$$

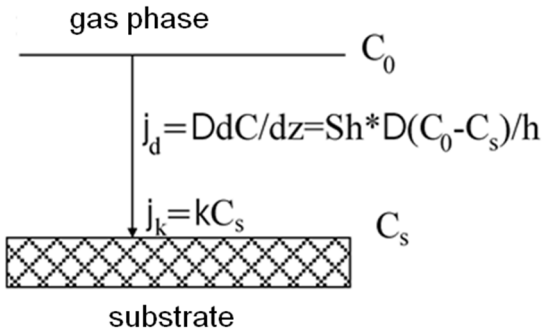

$$\frac{1}{j} = \frac{1}{j_d} + \frac{1}{j_k}$$

Fig.10. Schematic representation of kinetics of MOCVD process and temperature dependence of deposition rate.

Sh – Sherwood number:

$$\mathrm{Sh} = \frac{KL}{D} = \frac{\text{Convective mass transfer coefficient}}{\text{Diffusive mass transfer coefficient}}$$

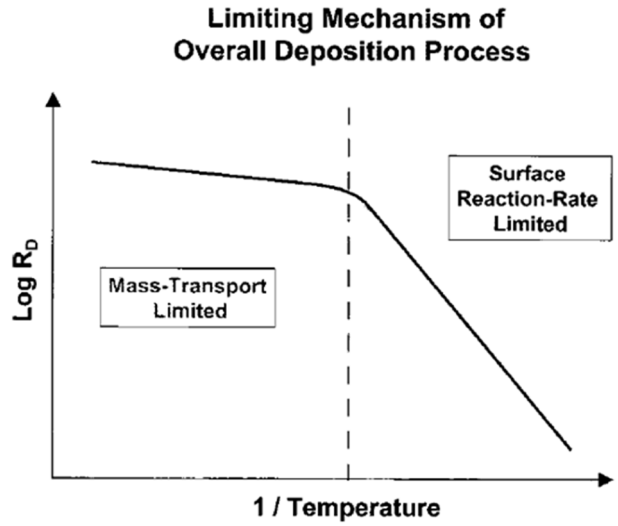

Fig.10. Schematic diagram showing the expected deposition rate behavior for a generic CVD process as a function of temperature. Shown on the diagram are the two limiting regimes typically encountered in a CVD process.[John E. Crowell, J. Vac. Sci. Technol. A 21(5) 2003]

1.5.d. *PECVD (plasma enhanced CVD), APCVD (atmospheric pressure CVD), water assisted CVD*

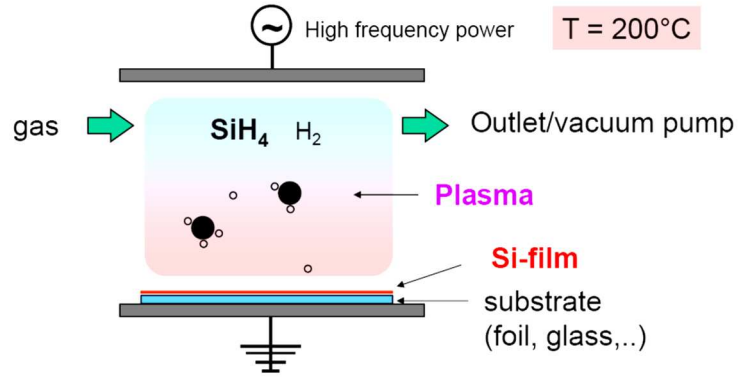

Fig. 8. PECVD-process of silicon. CVD principle: gas is activated/dissociated by the plasma (plasma potential rather small / no sputtering).

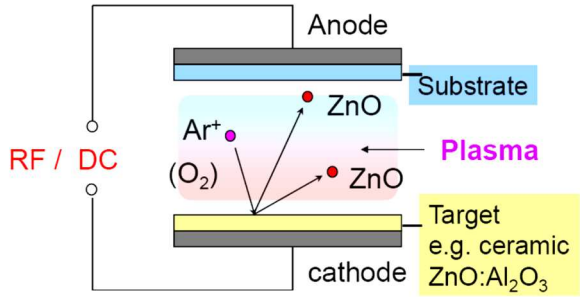

Fig. 9. Sputter-process for ZnO deposition. Sputter principle: heavy ions (Ar) are accelerated by the plasma potential and sputter atoms.

1.6. Overview of other vacuum methods

1.6.a. *PLD (pulsed laser deposition)*

1.6.b. *Texture generating methods: ISD (inclined substrate deposition), IBAD (ion beam assisted deposition)*

Special PVD: ISD in general a is not equal to b, but it determins b.

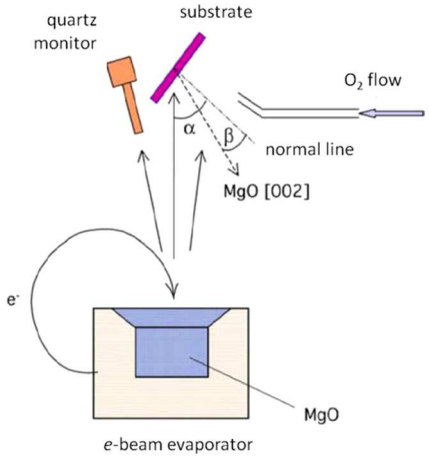

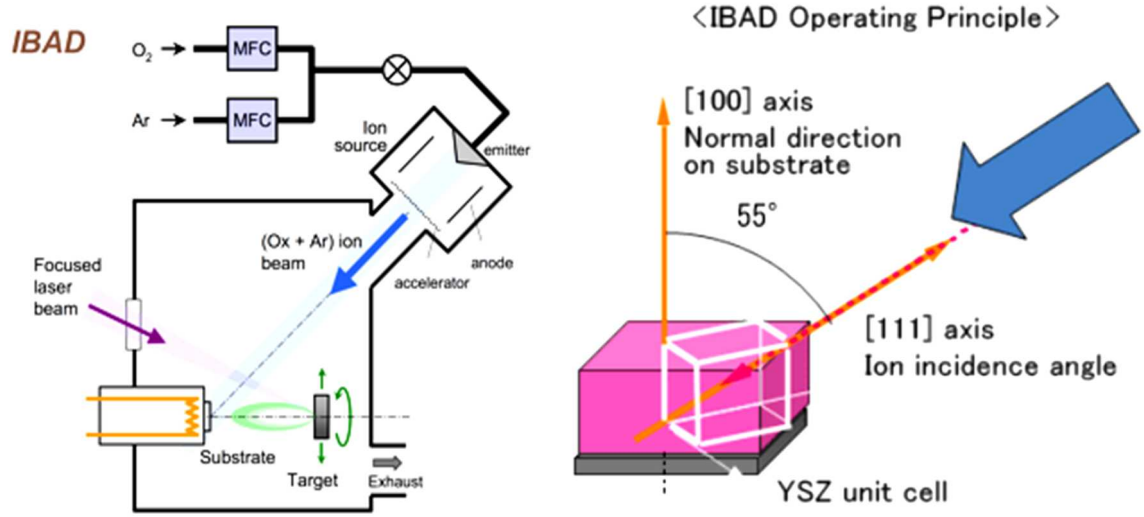

1.6.c. *ALD (atomic layer deposition)*

1.7. Overview of some wet-chemical methods (sol-gel, spray pyrolysis, ink-jet printing, spin-coating, dip-coating)

2. Overview of some important instrumental analytics for thin films.

	EPMA	AES	XPS	SIMS
Primary Secondary	Electrons (X-ray) Photons	Electrons (Auger) Electrons	(X-ray) Photons (Photo) Electrons	Ions Ions
Depth Resolution Lateral Resolution	200 nm 0.5 µm	2 nm 0.05 µm	2 nm 300 µm	2 nm 0.2 µm
Elements Limit of detection Quantification	Be-U 10E-4 At% ±2% rel.	Li-U 10E-1At% ±10% rel.	Li-U 10E-1 At% ±10% rel.	H-U 10E-7At% ±20% rel.
Depth Profiling	Cross Sections	Sputtering	Sputtering	Sputtering
Materials	All	Insulators difficult	All	All
Special Applications	SEM-Imaging	SEM-Imaging	Binding Structure (Surface)	Isotope Analysis Molecular Analysis

Fig. 9. Overview of analytical methods for chemical analysis of thin films.

2.1. XRD (X-Ray Diffraction)

Crystal structure

Johannes Kepler hypothesized in his work Strena seu de Nive Sexangula (A New Year's Gift of Hexagonal Snow) (1611) that the hexagonal symmetry of snowflake crystals was due to a regular packing of spherical water particles. Danish scientist Nicolas Steno (1669) had showed that the angles between the faces are the same in every exemplar of a particular type of crystal. *René Just Haüy* (1784) had discovered that every face of a crystal can be described by simple stacking patterns of blocks of the same shape and size.

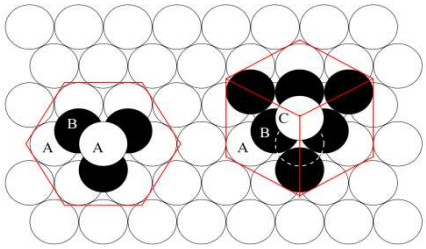

Crystal systems

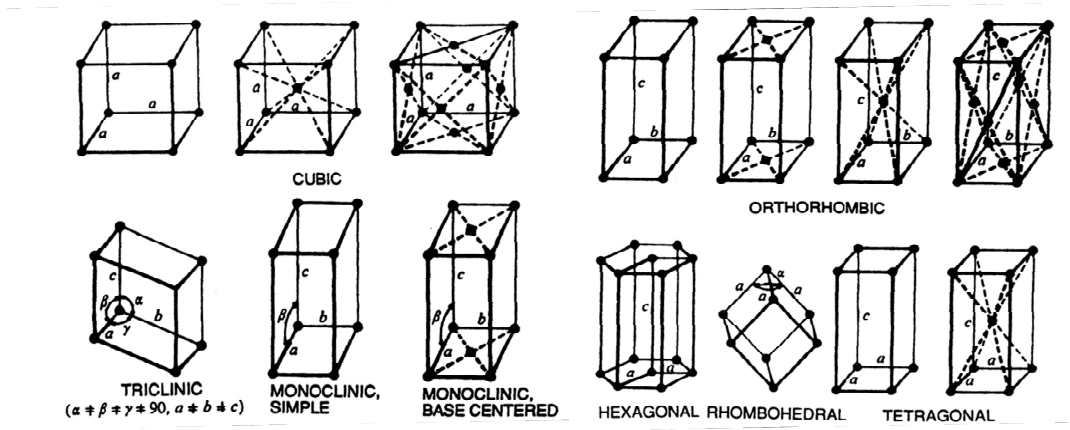

Miller indices: cubic lattice

William Hallowes Miller in 1839 was able to give each face a unique label of three small integers, the Miller indices which are still used today for identifying crystal faces.

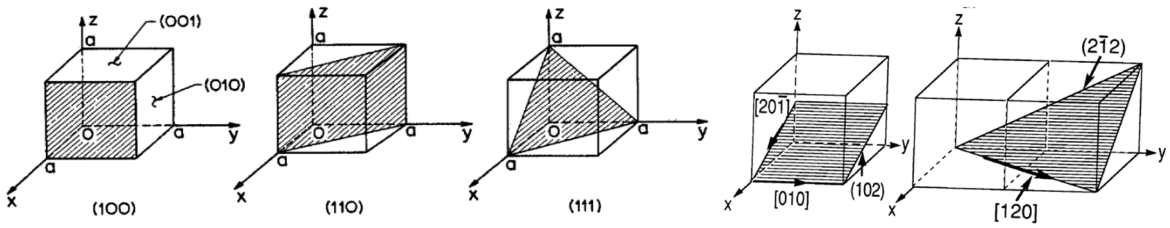

Fig. 10. Miller indices h, k, l: determine intercepts of the plane with the three basis axes in terms of lattice constants - take the reciprocals of the numbers and reduce them to the smallest three integers having the same ratio.

(*hkl*) – plane
{*hkl*} - family of planes
[*hkl*] - direction

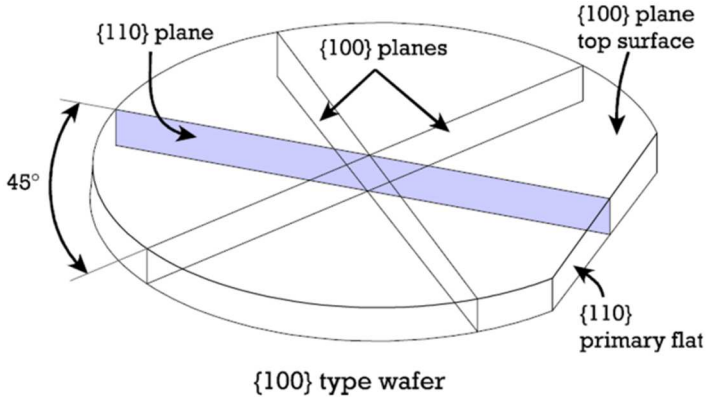

Fig. 10. Si-wafer.

Miller indices: hexagonal lattice

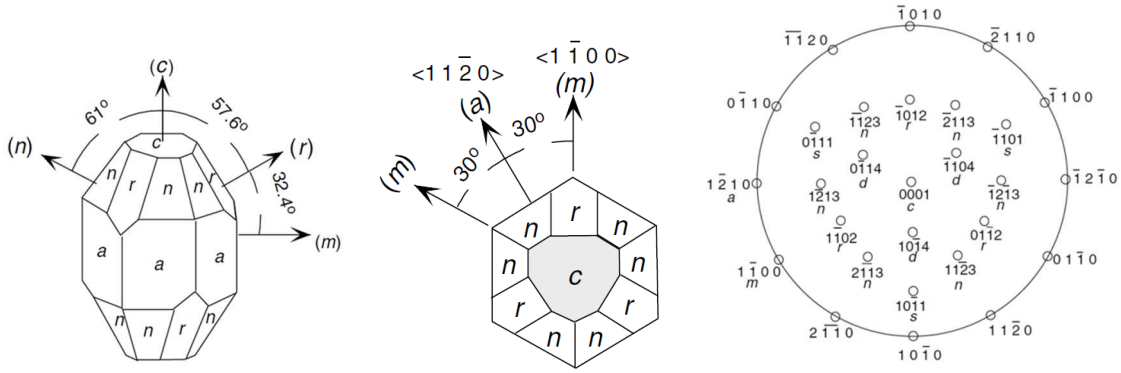

Fig. 10. Labeling of planes in hexagonal symmetry (for sapphire).

X-rays: properties

X-rays were discovered by *Wilhelm Conrad Röntgen* in 1895, just as the studies of crystal symmetry were being concluded.

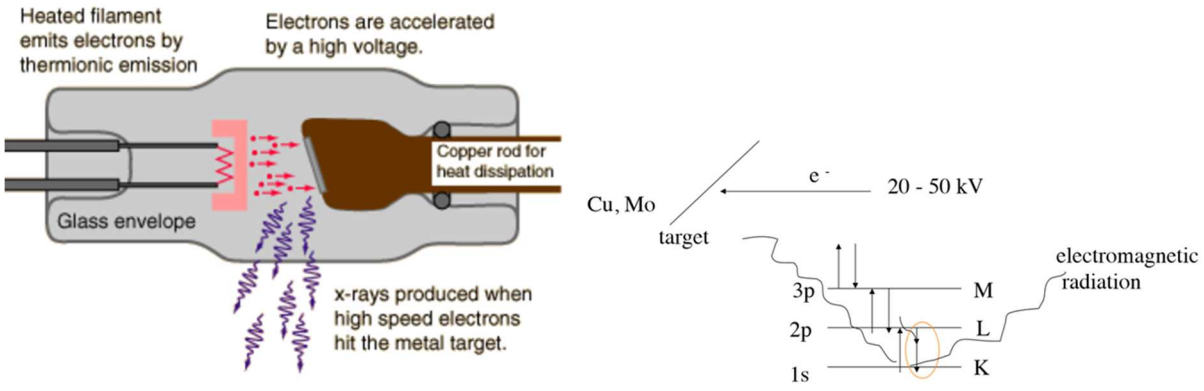

Broad background is called Bremsstrahlung. Electrons are slowed down and loose energy in the form of X-rays. X-rays range in wavelength from 10 to 0,01 nanometers; a typical wavelength used for crystallography is 1 Å (0,1 nm), which is on the scale of covalent chemical bonds and the radius of a single atom.

X-rays interact with the atoms in a crystal.

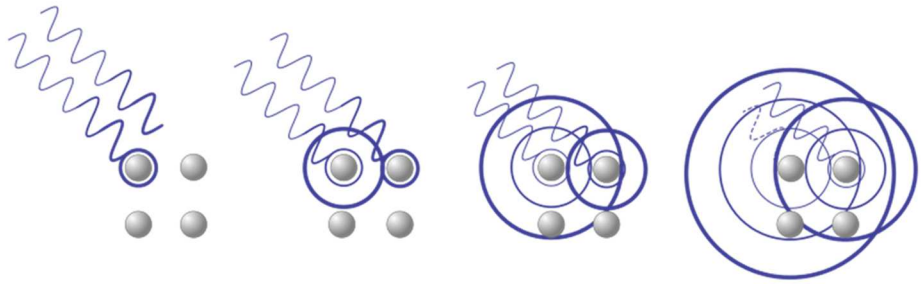

Fig. 10. X-ray crystallography is a form of elastic scattering; the outgoing X-rays have the same energy, and thus same wavelength, as the incoming X-rays, only with altered direction.

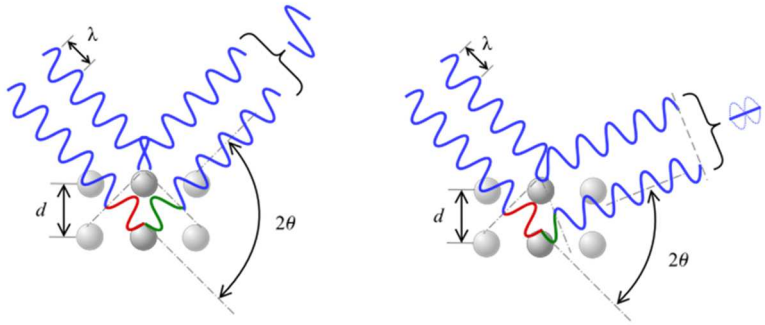

Fig. 10. According to the 2θ deviation, the phase shift causes constructive (left figure) or destructive (right figure) interferences.

It was proposed that the incident X-ray radiation would produce a peak if their reflections off the various planes interfered constructively. W. L. Bragg had modelled the crystal as a set of discrete parallel planes separated by a constant parameter *d*. The interference is constructive when the phase shift is an integer number of the wavelength.

Bragg's Law: $2d\sin\theta = n\lambda$

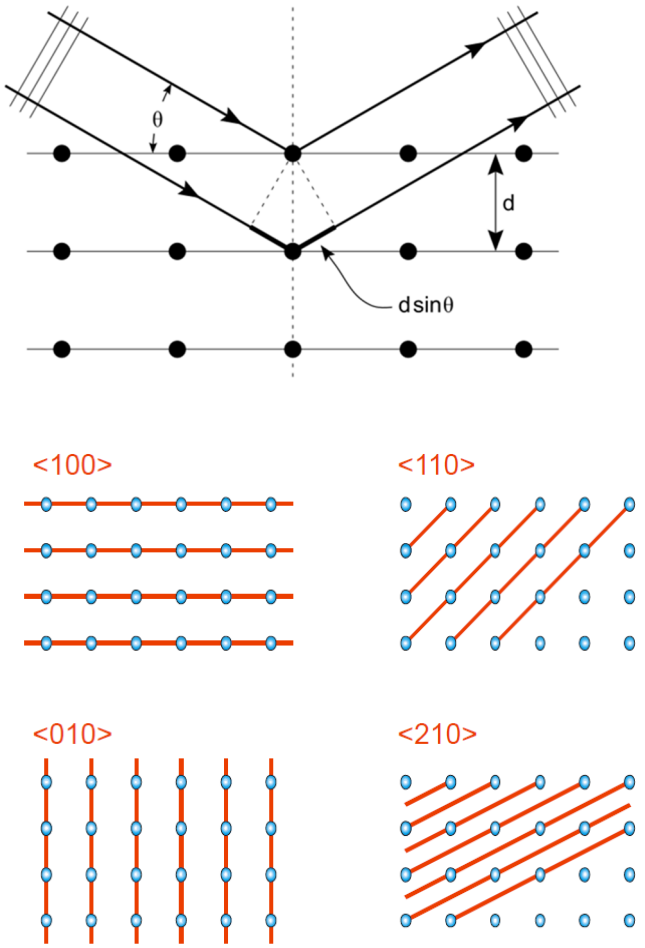

Fig. 10. X-ray patterns. *The number is large but finite, if theta = 90°, then d = λ/2. For Cu radiation that means that we can only see d-spacings down to 0.77 Å, for Mo radiation, down to about 0.35 Å.*

The **Scherrer equation** can be written as:

$$\tau = \frac{K\lambda}{\beta \cos\theta}$$

where:

- ***t*** is the mean size of the ordered (crystalline) domains, which may be smaller or equal to the grain size;
- ***K*** is a dimensionless **shape factor**, with a value close to unity. The shape factor has a typical value of about 0.9, but varies with the actual shape of the crystallite;
- ***λ*** is the X-ray wavelength;
- ***β*** is the line broadening at half the maximum intensity (FWHM), after subtracting the instrumental line broadening, in radians. This quantity is also sometimes denoted as $\Delta(2\theta)$;
- ***θ*** is the Bragg angle.

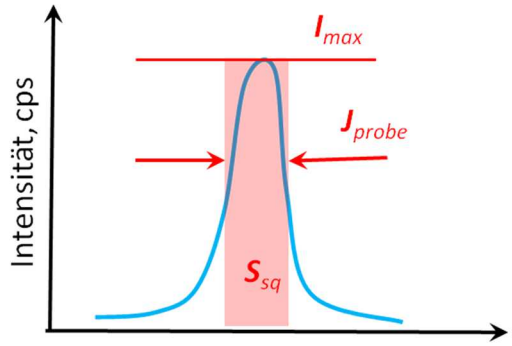

Fig. 10.

$J_{\text{net probe}} = J_{\text{probe}} - J_{\text{stand}}$
(e.g. LaB_6 – standard)
$\beta = J_{\text{net probe}}$ (rad)

Line Broadening Analysis: Deviations from ideal crystallinity, such as finite crystallite size and strain (at the atomic level) lead to broadening of the diffraction lines. By analyzing this broadening it is possible to extract information about the microstructure of a material.

Sources of Line Broadening:

- Instrumental Broadening
- Crystallite Size Broadening
- Strain Broadening

Methods of Analysis:

- Simplified Integral Breadth Methods
- Fourier Methods
- Double Voigt Methods

A perfect crystal would extend in all directions to infinity, so we can say that no crystal is perfect due to it.s finite size. This deviation from perfect crystallinity leads to a roadening of the diffraction peaks. However, above a certain size (~0.1 - 1 micron) this type of broadening is negligible. Crystallite size is a measure of the size of a coherently diffracting domain. Due to the presence of polycrystalline aggregates crystallite size is not generally the same thing as particle size. Other techniques for measuring size, measure the particle size rather than the crystallite size. BET, Light (Laser) Scattering, . Electron Microscopy (SEM).

Extended defects disrupt the atomic arrangement of a crystal, typically along a 2D plane. These defects effectively terminate a crystallographically ordered domain of the crystal. Thus as far as x-rays are concerned one crystal ends and a new crystal begins at the extended defect. Crystallite size analysis on a sample containing extended defects can be used to estimate the ordered domain size (the size of the region between defects) in the same manner that XRD is used to determine crystallite size.

- Types of extended defects:
- Stacking faults (ABCABCABCCBACBACBA)
- Dislocations in layered materials (graphite, MoS2, clays, ZrNCl, etc.)

- Antiphase boundaries, which arise in partially ordered

materials (Cu3Au, Sr2AlTaO6)

2.1. a. *Texture analysis, determination of sizes of coherent scattering areas.*

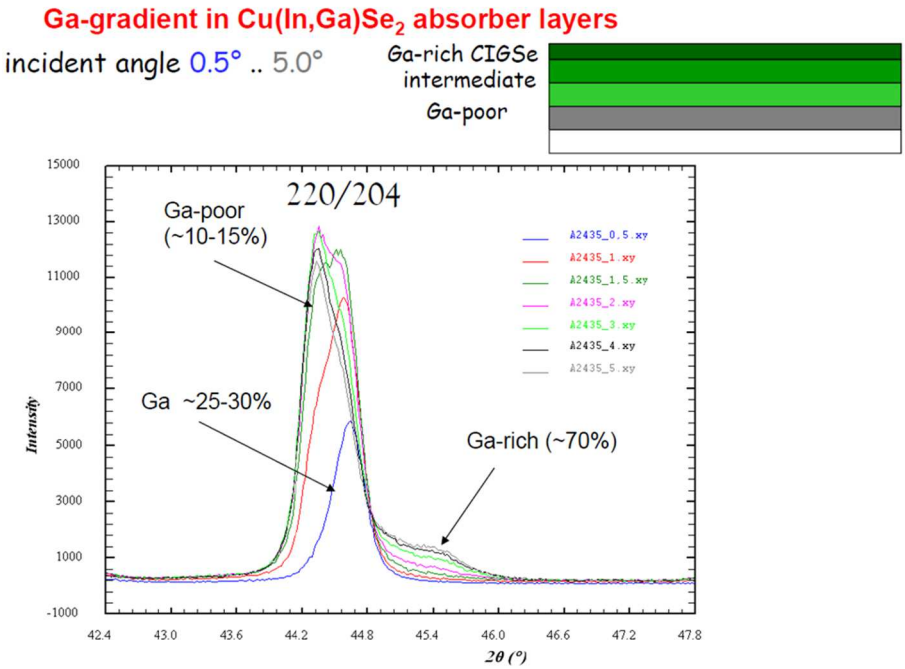

Fig. 10. Phase analysis – case study: Ga^{3+} (VI) has smaller ionic radius as In^{3+} (VI), namely 0.62 Å vs 0.8 Å,that is the reason of different lattice constants and, hence, different 2θ providing the constructive interference.In general: bigger lattice constant ->-> smaller 2θ of the peak position

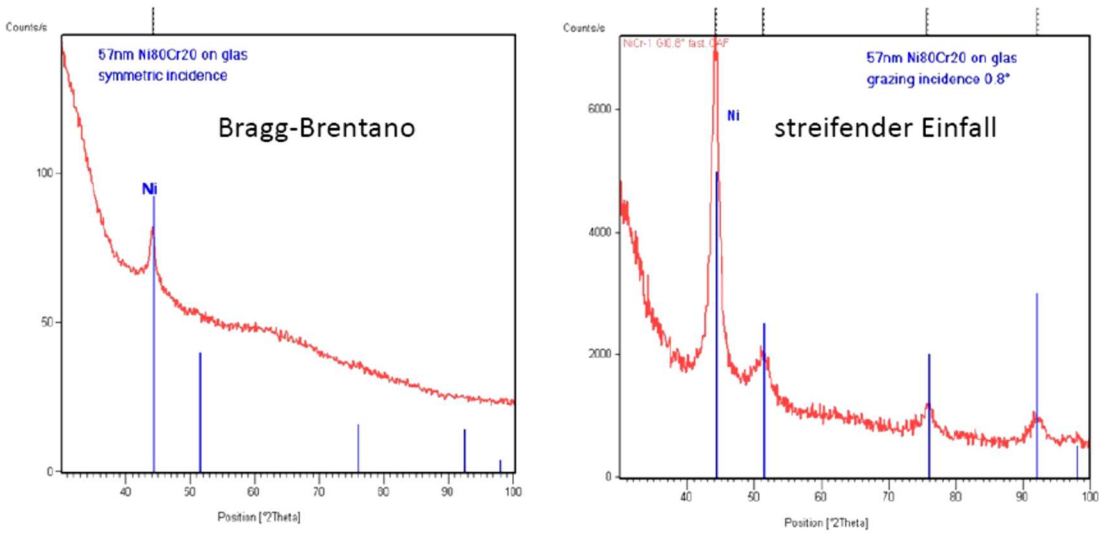

Fig. 9.Phase analysis of very thin films by grazing incidence. Example: 57 nm $Ni_{80}Cr_{20}$ on glass.

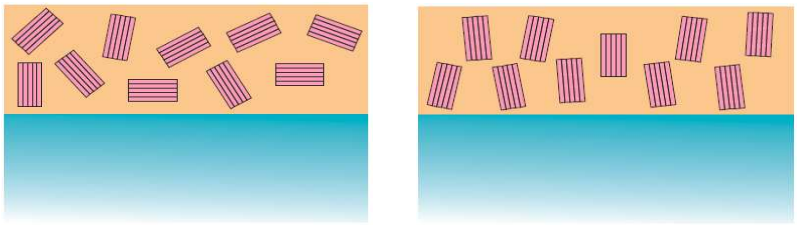

nontexturred polycristalline film **texturred polycristalline film**

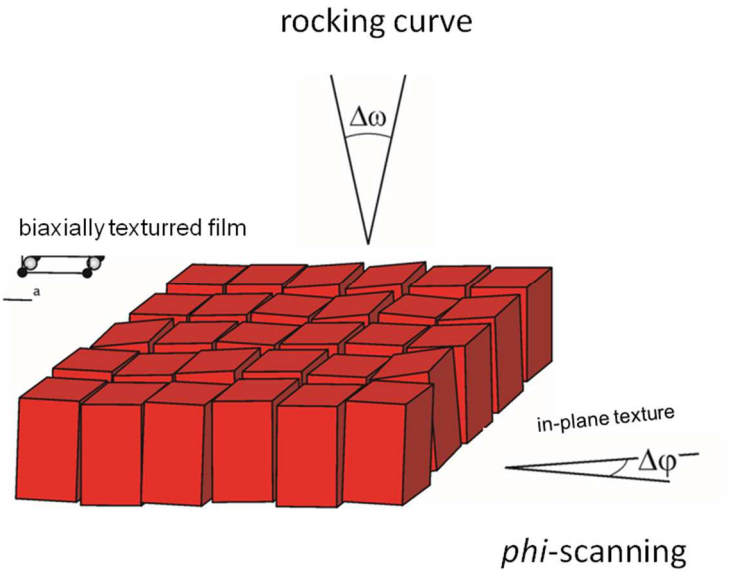

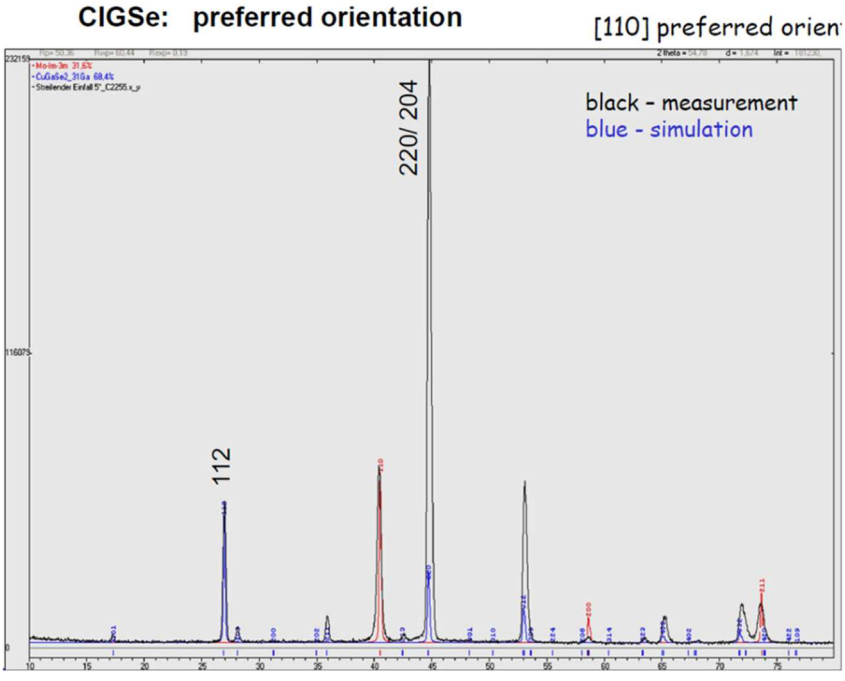

2.1.b. *Determination of stresses in the film.*

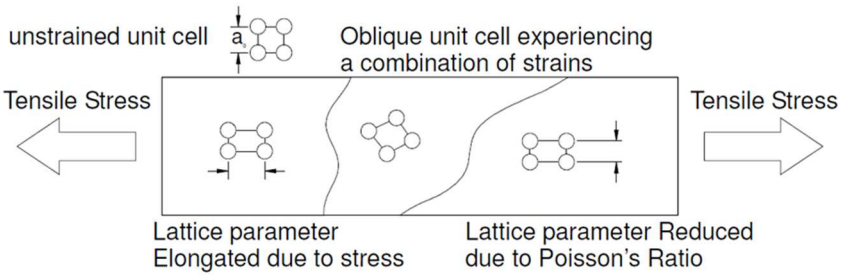

Fig. 10. Stress analysis

Since this stress is in a thin film, and therefore near the surface, the normal stress in the z-direction will not exist. ε_x component of the 3D-Strain Transformation to the ε_x' Axis.

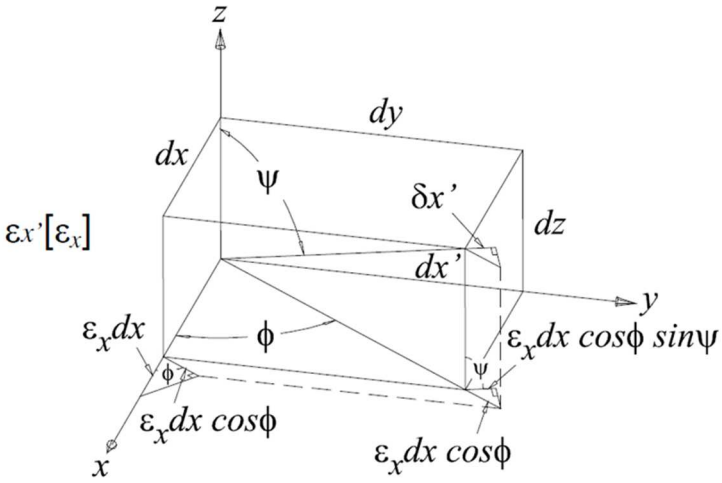

$$\varepsilon_{\phi\psi} = \frac{d_{\phi\psi} - d_0}{d_0} = \frac{1+\nu}{E}\sigma_\phi \sin^2\psi - \frac{2\nu}{E}(\sigma_x + \sigma_y) + \frac{1+\nu}{E}(\tau_{xz}\cos\phi + \tau_{yz}\sin\phi)\sin 2\psi$$

E is the elastic modulus of the film, is Poisson's ratio of the film, and d0 is the unstrained lattice parameter.

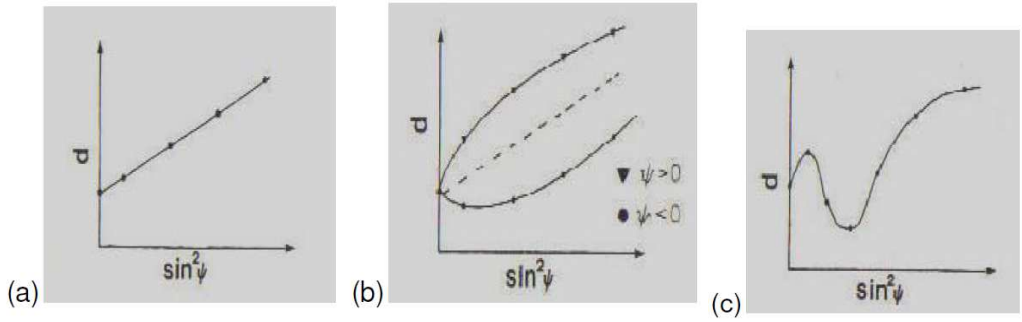

$d_{\phi\psi}$ vs. $\mathrm{Sin}^2\psi$ for (a) Linear Behavior, (b) ψ-Splitting Behavior, and (c) Oscillatory Behavior.

If shear stresses τ_{xz}, and τ_{yz} are zero, then the dependence will have a linear behavior with $\sin^2\psi$. If the shear stresses are non-zero, the plot of $d_{\phi\psi}$ vs. $\sin^2\psi$ will have a – splitting behavior. If the plot of $d_{\phi\psi}$ vs. $\sin^2\psi$ shows an oscillatory behavior it indicates that the material is textured and strain cannot be solved using equations mentioned
above

Lattice Strain (Microstrain)

Strain is a term used more often in engineering than in chemistry. Strain is defined as the deformation of an object divided by it s ideal length, $\Delta d/d$. In crystals there we can observe two types of strain: Uniform strain and Non-uniform strain.

Uniform strain causes the unit cell to expand/contract in an isotropic way. This simply leads to a change in the unit cell parameters and shift of the peaks. There is no broadening associated with this type of strain. Non-uniform strain leads to systematic shifts of atoms from their ideal positions and to peak broadening. This type of strain arises from the following sources:

- Point defects (vacancies, site-disorder)
- Plastic deformation (cold worked metals, thin films)
- Poor crystallinity

Strain Broadening

Stokes and Wilson (1944) first observed that strained or imperfect crystals containing line broadening of a different sort, than the broadening that arises from small crystallite size.

$\varepsilon str = \beta/\{4 \tan \theta\}$

εstr = weighted average strain

β = The integral breadth of a reflection (in radians 2θ) located at 2θ.

Note that size and strain broadening show a different θ dependence. This provides a way to separate the two effects.

Williamson-Hall Analysis

Simplified Integral Breadth Methods

Williamson and Hall (1953) proposed a method for deconvoluting size and strain broadening by looking at the peak width as a function of 2θ. Here I derive the Williamson-Hall relationship for the Lorentzian peak shape, but it can derived in a similar manner for the Gaussian peak shape

$\{\beta obs - \beta inst\} = \lambda/\{Dv \cos \theta\} + 4\, \varepsilon str\{\tan \theta\}$

$\{\beta obs - \beta inst\} \cos \theta = \lambda/Dv + 4\, \varepsilon str\{\sin \theta\}$

To make a Williamson-Hall plot

- Plot $\{\beta obs - \beta inst\} \cos \theta$ on the y-axis (in radians 2θ)
- Plot $4 \sin\theta$ on the x-axis

If you get a linear fit to the data you can extract

- the crystallite size from the y-intercept of the fit
- the strain from the slope of the fit

Size-Strain Analysis from Rietveld Profile Parameters

If we look at the Lorentzian and Gaussian terms in the Thompson-Cox-Hastings pseudo-voigt function (GSAS reverses the definition of X and Y from the original work I think) we can see how size and strain parameters can be extracted from the refined profile parameters [see also P. Karen & P.M. Woodward, J. Solid State Chem. 141, 78-88 (1998)].

Lorentzian TCH Function

$\Gamma L = X/(\cos\theta) + Y \tan\theta$

W-H Analysis

$\{\beta obs - \beta inst\} = \lambda/\{Dv\cos\theta\} + 4\,\varepsilon str\{\tan\theta\}$

Correcting for FWHM vs. Integral breadth, and realizing that GSAS counts steps in centidegrees we can come up Size and Strain from X and Y

$Dv = 36000\,\lambda/\{\pi 2\,X\}$

$\varepsilon str = \pi 2\,\{Y\text{-}Yinst\}/144000$

Fourier Methods

The most accurate way of extracting size and strain information is to analyze the entire shape of several reflections in the pattern (ideally higher order reflections of the same type I.e. 100, 200, 300, etc. or 111, 222, 333, etc.), by the method developed by Warren and Averbach [J. Appl. Phys. 21, 596 (1950).] This is done using the following steps:

- Fit each reflection of interest with a Fourier series.
- Repeat this procedure for a pattern of a sample which gives no broadening, in order to determine the instrumental contribution to broadening.
- Use these results to deconvolute the sample broadening from the instrumental broadening, via a Stokes Fourier deconvolution.
- Extract information regarding the size distribution and strain profile by analyzing the theta dependence of the cosine Fourier coefficients (which describe the symmetric broadening).

2.1.c. *Determination of crystalline, polycrystalline and amorphous parts of the film.*

2.2. Electron diffraction methods: EBSD, RHEED/LEED.

2.3. Analysis of composition: EDX/EPMA, XPS.

2.4. Analysis of microstructure: SEM, AFM

3. Superconductive wires.

3.1. Superconductivity phenomenon, history, materials.

Superconductivity is a phenomenon of exactly zero electrical resistance and expulsion of magnetic fields occurring in certain materials when cooled below a characteristic critical temperature. It was discovered by Dutch physicist Heike Kamerlingh Onnes on April 8, 1911 in Leiden. Like ferromagnetism and atomic spectral lines, superconductivity is a quantum mechanical phenomenon. It is characterized by the Meissner effect, the complete ejection of magnetic field lines from the interior of the superconductor as it transitions into the superconducting state. The occurrence of the Meissner effect indicates that superconductivity cannot be understood simply as the idealization of perfect conductivity in classical physics.

The electrical resistivity of a metallic conductor decreases gradually as temperature is lowered. In ordinary conductors, such as copper or silver, this decrease is limited by impurities and other defects. Even near absolute zero, a real sample of a normal conductor shows some resistance. In a superconductor, the resistance drops abruptly to zero when the material is cooled

below its critical temperature. An electric current flowing through a loop of superconducting wire can persist indefinitely with no power source.*[Durrant, Alan (2000). Quantum Physics of Matter. CRC Press. pp. 102–103. ISBN 0750307218.]*

In 1986, it was discovered that some cuprate-perovskite ceramic materials have a critical temperature above 90 K (−183 °C)*.[J. G. Bednorz and K. A. Müller (1986). "Possible high T_c superconductivity in the Ba−La−Cu−O system". Z. Physik, B **64** (1): 189–193.]* Such a high transition temperature is theoretically impossible for a conventional superconductor, leading the materials to be termed high-temperature superconductors. Liquid nitrogen boils at 77 K, and superconduction at higher temperatures than this facilitates many experiments and applications that are less practical at lower temperatures.

There are many criteria by which superconductors are classified. The most common are:

- **Response to a magnetic field:** A superconductor can be Type I, meaning it has a single critical field, above which all superconductivity is lost; or Type II, meaning it has two critical fields, between which it allows partial penetration of the magnetic field.
- **By theory of operation:** It is conventional if it can be explained by the BCS theory or its derivatives, or unconventional, otherwise.
- **By critical temperature:** A superconductor is generally considered high temperature if it reaches a superconducting state when cooled using liquid nitrogen – that is, at only Tc > 77 K) – or low temperature if more aggressive cooling techniques are required to reach its critical temperature.
- **By material:** Superconductor material classes include chemical elements (e.g. mercury or lead), alloys (such as niobium-titanium, germanium-niobium, and niobium nitride), ceramics (YBCO and magnesium diboride), or organic superconductors (fullerenes and carbon nanotubes; though perhaps these examples should be included among the chemical elements, as they are composed entirely of carbon).

3.2. 1st and 2nd generation (G) of high temperature superconductive (HTS) wires.

3.2.a. *Comparison of superconductive materials and concepts used in 1G and 2G-HTS-wires.*

Most of the physical properties of superconductors vary from material to material, such as the heat capacity and the critical temperature, critical field, and critical current density at which superconductivity is destroyed.

On the other hand, there is a class of properties that are independent of the underlying material. For instance, all superconductors have exactly zero resistivity to low applied currents when there is no magnetic field present or if the applied field does not exceed a critical value. The existence of these "universal" properties implies that superconductivity is a thermodynamic phase, and thus possesses certain distinguishing properties which are largely independent of microscopic details.

Zero electrical DC resistance

The simplest method to measure the electrical resistance of a sample of some material is to place it in an electrical circuit in series with a current source I and measure the resulting voltage V across the sample. The resistance of the sample is given by Ohm's law as R = V / I. If the voltage is zero, this means that the resistance is zero.

Superconductors are also able to maintain a current with no applied voltage whatsoever, a property exploited in superconducting electromagnets such as those found in MRI machines.

Experiments have demonstrated that currents in superconducting coils can persist for years without any measurable degradation. Experimental evidence points to a current lifetime of at least 100,000 years. Theoretical estimates for the lifetime of a persistent current can exceed the estimated lifetime of the universe, depending on the wire geometry and the temperature.

In a normal conductor, an electric current may be visualized as a fluid of electrons moving across a heavy ionic lattice. The electrons are constantly colliding with the ions in the lattice, and during each collision some of the energy carried by the current is absorbed by the lattice and converted into heat, which is essentially the vibrational kinetic energy of the lattice ions. As a result, the energy carried by the current is constantly being dissipated. This is the phenomenon of electrical resistance.

The situation is different in a superconductor. In a conventional superconductor, the electronic fluid cannot be resolved into individual electrons. Instead, it consists of bound pairs of electrons known as Cooper pairs. This pairing is caused by an attractive force between electrons from the exchange of phonons. Due to quantum mechanics, the energy spectrum of this Cooper pair fluid possesses an energy gap, meaning there is a minimum amount of energy ΔE that must be supplied in order to excite the fluid. Therefore, if ΔE is larger than the thermal energy of the lattice, given by kT, where k is Boltzmann's constant and T is the temperature, the fluid will not be scattered by the lattice. The Cooper pair fluid is thus a superfluid, meaning it can flow without energy dissipation.

In a class of superconductors known as type II superconductors, including all known high-temperature superconductors, an extremely small amount of resistivity appears at temperatures not too far below the nominal superconducting transition when an electric current is applied in conjunction with a strong magnetic field, which may be caused by the electric current. This is due to the motion of magnetic vortices in the electronic superfluid, which dissipates some of the energy carried by the current. If the current is sufficiently small, the vortices are stationary, and the resistivity vanishes. The resistance due to this effect is tiny compared with that of non-superconducting materials, but must be taken into account in sensitive experiments. However, as the temperature decreases far enough below the nominal superconducting transition, these vortices can become frozen into a disordered but stationary phase known as a "vortex glass". Below this vortex glass transition temperature, the resistance of the material becomes truly zero.

Superconducting phase transition

In superconducting materials, the characteristics of superconductivity appear when the temperature T is lowered below a critical temperature Tc. The value of this critical temperature varies from material to material. Conventional superconductors usually have critical temperatures ranging from around 20 K to less than 1 K. Solid mercury, for example, has a critical temperature of 4.2 K. As of 2009, the highest critical temperature found for a conventional superconductor is 39 K for magnesium diboride (MgB2),[7][8] although this material displays enough exotic properties that there is some doubt about classifying it as a "conventional" superconductor.[9] Cuprate superconductors can have much higher critical temperatures: YBa2Cu3O7, one of the first cuprate superconductors to be discovered, has a critical temperature of 92 K, and mercury-based cuprates have been found with critical temperatures in excess of 130 K. The explanation for these high critical temperatures remains unknown. Electron pairing due to phonon exchanges explains superconductivity in

conventional superconductors, but it does not explain superconductivity in the newer superconductors that have a very high critical temperature.

Similarly, at a fixed temperature below the critical temperature, superconducting materials cease to superconduct when an external magnetic field is applied which is greater than the critical magnetic field. This is because the Gibbs free energy of the superconducting phase increases quadratically with the magnetic field while the free energy of the normal phase is roughly independent of the magnetic field. If the material superconducts in the absence of a field, then the superconducting phase free energy is lower than that of the normal phase and so for some finite value of the magnetic field (proportional to the square root of the difference of the free energies at zero magnetic field) the two free energies will be equal and a phase transition to the normal phase will occur. More generally, a higher temperature and a stronger magnetic field lead to a smaller fraction of the electrons in the superconducting band and consequently a longer London penetration depth of external magnetic fields and currents. The penetration depth becomes infinite at the phase transition.

The onset of superconductivity is accompanied by abrupt changes in various physical properties, which is the hallmark of a phase transition. For example, the electronic heat capacity is proportional to the temperature in the normal (non-superconducting) regime. At the superconducting transition, it suffers a discontinuous jump and thereafter ceases to be linear. At low temperatures, it varies instead as $e^{-\alpha/T}$ for some constant, α. This exponential behavior is one of the pieces of evidence for the existence of the energy gap.

The order of the superconducting phase transition was long a matter of debate. Experiments indicate that the transition is second-order, meaning there is no latent heat. However in the presence of an external magnetic field there is latent heat, because the superconducting phase has a lower entropy below the critical temperature than the normal phase. It has been experimentally demonstrated[10] that, as a consequence, when the magnetic field is increased beyond the critical field, the resulting phase transition leads to a decrease in the temperature of the superconducting material.

Calculations in the 1970s suggested that it may actually be weakly first-order due to the effect of long-range fluctuations in the electromagnetic field. In the 1980s it was shown theoretically with the help of a disorder field theory, in which the vortex lines of the superconductor play a major role, that the transition is of second order within the type II regime and of first order (i.e., latent heat) within the type I regime, and that the two regions are separated by a tricritical point.[11] The results were strongly supported by Monte Carlo computer simulations.[12]

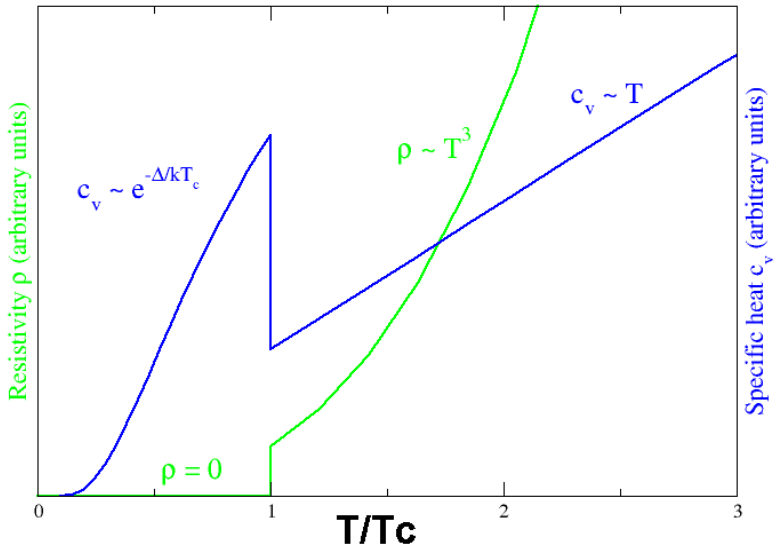

Fig. 10. Behavior of heat capacity (c_v, blue) and resistivity (ρ, green) at the superconducting phase transition

Meissner effect

When a superconductor is placed in a weak external magnetic field H, and cooled below its transition temperature, the magnetic field is ejected. The Meissner effect does not cause the field to be completely ejected but instead the field penetrates the superconductor but only to a very small distance, characterized by a parameter λ, called the London penetration depth, decaying exponentially to zero within the bulk of the material. The Meissner effect is a defining characteristic of superconductivity. For most superconductors, the London penetration depth is on the order of 100 nm.

The Meissner effect is sometimes confused with the kind of diamagnetism one would expect in a perfect electrical conductor: according to Lenz's law, when a changing magnetic field is applied to a conductor, it will induce an electric current in the conductor that creates an opposing magnetic field. In a perfect conductor, an arbitrarily large current can be induced, and the resulting magnetic field exactly cancels the applied field.

The Meissner effect is distinct from this—it is the spontaneous expulsion which occurs during transition to superconductivity. Suppose we have a material in its normal state, containing a constant internal magnetic field. When the material is cooled below the critical temperature, we would observe the abrupt expulsion of the internal magnetic field, which we would not expect based on Lenz's law.

The Meissner effect was given a phenomenological explanation by the brothers Fritz and Heinz London, who showed that the electromagnetic free energy in a superconductor is minimized provided

$$\nabla^2 \mathbf{H} = \lambda^{-2} \mathbf{H}$$

where H is the magnetic field and λ is the London penetration depth.

This equation, which is known as the London equation, predicts that the magnetic field in a superconductor decays exponentially from whatever value it possesses at the surface.

A superconductor with little or no magnetic field within it is said to be in the Meissner state. The Meissner state breaks down when the applied magnetic field is too large. Superconductors can be divided into two classes according to how this breakdown occurs. In Type I superconductors, superconductivity is abruptly destroyed when the strength of the applied field

rises above a critical value Hc. Depending on the geometry of the sample, one may obtain an intermediate state[13] consisting of a baroque pattern[14] of regions of normal material carrying a magnetic field mixed with regions of superconducting material containing no field. In Type II superconductors, raising the applied field past a critical value Hc1 leads to a mixed state (also known as the vortex state) in which an increasing amount of magnetic flux penetrates the material, but there remains no resistance to the flow of electric current as long as the current is not too large. At a second critical field strength Hc2, superconductivity is destroyed. The mixed state is actually caused by vortices in the electronic superfluid, sometimes called fluxons because the flux carried by these vortices is quantized. Most pure elemental superconductors, except niobium and carbon nanotubes, are Type I, while almost all impure and compound superconductors are Type II.

London moment

Conversely, a spinning superconductor generates a magnetic field, precisely aligned with the spin axis. The effect, the London moment, was put to good use in Gravity Probe B. This experiment measured the magnetic fields of four superconducting gyroscopes to determine their spin axes. This was critical to the experiment since it is one of the few ways to accurately determine the spin axis of an otherwise featureless sphere.

High-temperature superconductivity

Until 1986, physicists had believed that BCS theory forbade superconductivity at temperatures above about 30 K. In that year, Bednorz and Müller discovered superconductivity in a lanthanum-based cuprate perovskite material, which had a transition temperature of 35 K (Nobel Prize in Physics, 1987).[6] It was soon found that replacing the lanthanum with yttrium (i.e., making YBCO) raised the critical temperature to 92 K.[32]

This temperature jump is particularly significant, since it allows liquid nitrogen as a refrigerant, replacing liquid helium.[32] This can be important commercially because liquid nitrogen can be produced relatively cheaply, even on-site, avoiding some of the problems (such as so-called "solid air" plugs) which arise when liquid helium is used in piping.[33][34]

Many other cuprate superconductors have since been discovered, and the theory of superconductivity in these materials is one of the major outstanding challenges of theoretical condensed matter physics.[35] There are currently two main hypotheses – the resonating-valence-bond theory, and spin fluctuation which has the most support in the research community.[36] The second hypothesis proposed that electron pairing in high-temperature superconductors is mediated by short-range spin waves known as paramagnons.[37][38]

Since about 1993, the highest temperature superconductor was a ceramic material consisting of mercury, barium, calcium, copper and oxygen ($HgBa_2Ca_2Cu_3O_{8+\delta}$) with T_c = 133–138 K.[39][40] The latter experiment (138 K) still awaits experimental confirmation, however.

In February 2008, an iron-based family of high-temperature superconductors was discovered.[41][42] Hideo Hosono, of the Tokyo Institute of Technology, and colleagues found lanthanum oxygen fluorine iron arsenide ($LaO_{1-x}F_xFeAs$), an oxypnictide that superconducts below 26 K. Replacing the lanthanum in $LaO_{1-x}F_xFeAs$ with samarium leads to superconductors that work at 55 K.[43]

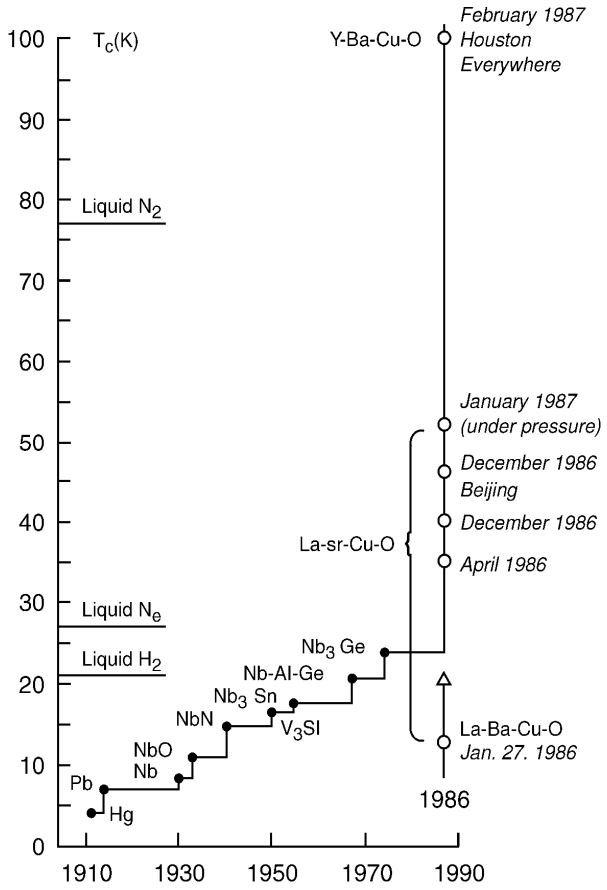

$La_{2-x}Ba_xCuO_{4-y}$ Nobel Prize in physics (1987) «For an important breackthrough in invention of superconductivity in ceramic materials» Alex Müller, Georg Bednorz .

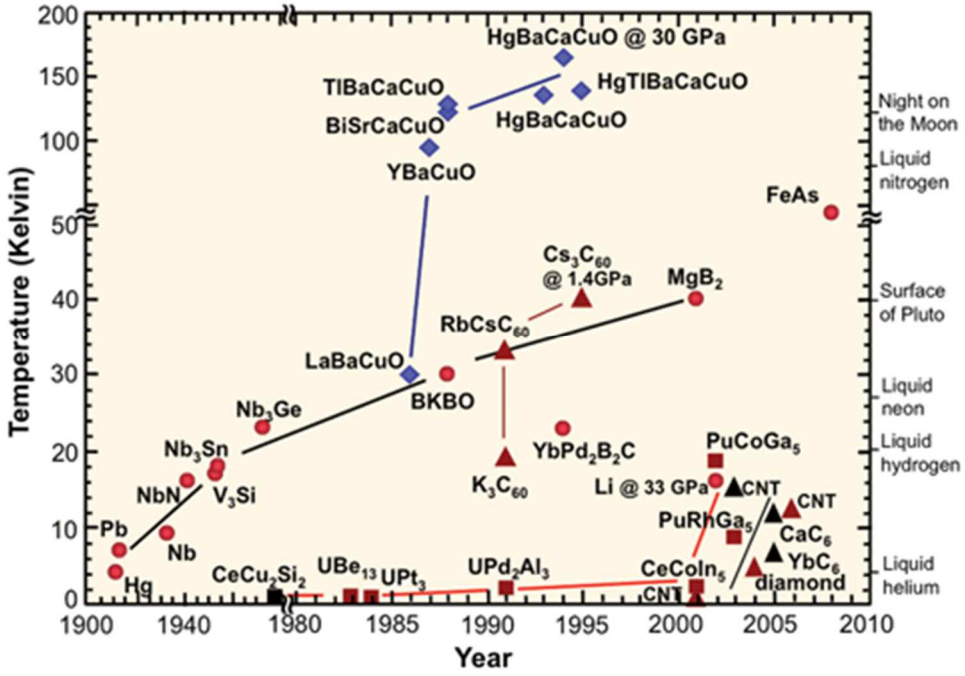

Fig. 10. Timeline of superconducting materials.

3.2.b. *Overview of fabrication technologies for 2G-HTSW.*

3.3. Application of HTS-Wires.

Some of the technological applications of superconductivity include:

- the production of sensitive magnetometers based on SQUIDs
- fast digital circuits (including those based on Josephson junctions and rapid single flux quantum technology),
- powerful superconducting electromagnets used in maglev trains, Magnetic Resonance Imaging (MRI) and Nuclear magnetic resonance (NMR) machines, magnetic confinement fusion reactors (e.g. tokamaks), and the beam-steering and focusing magnets used in particle accelerators
- low-loss power cables
- RF and microwave filters (e.g., for mobile phone base stations, as well as military ultra-sensitive/selective receivers)
- fast fault current limiters
- high sensitivity particle detectors, including the transition edge sensor, the superconducting bolometer, the superconducting tunnel junction detector, the kinetic inductance detector, and the superconducting nanowire single-photon detector
- railgun and coilgun magnets
- electric motors and generators[1]

3.3.a. *Awaited profit, cooling systems, very future technologies.*

According to AMSC (American Superconductor) estimations the use of HTS-coils will decrease compared to demagnetization coils made of Cu:

- the mass on 50-80%:
- energy consupmtion on 25%;
- costs on 75%;
- whole lenght of cables on more than 80%.

3.3.b. *Cables, FLCs (fault-current limiters).*

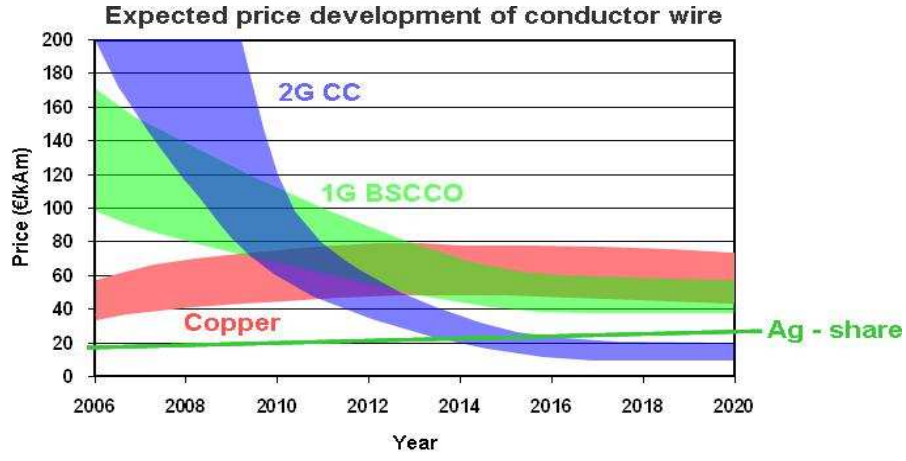

3.3.c. *Generators, motors.*

Expected HTS market development

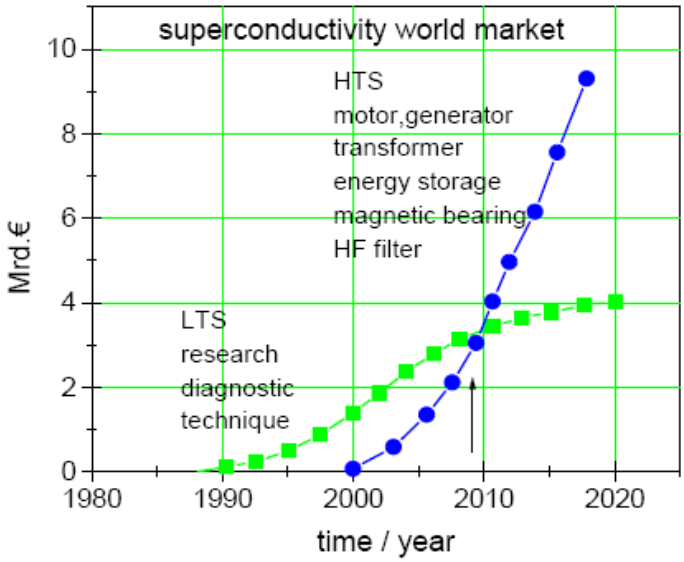

3.3.d. *Energy reserves, Inductive heaters.*

4. Photovoltaic

4.1. Basics and overview of existing technologies

Photovoltaics (PV) is a method of generating electrical power by converting sunlight into direct current electricity using semiconducting materials that exhibit the photovoltaic effect. A photovoltaic system employs solar panels composed of a number of solar cells to supply usable solar power. Power generation from solar PV has long been seen as a clean sustainable[1] energy technology which draws upon the planet's most plentiful and widely distributed renewable energy source – the sun. The direct conversion of sunlight to electricity occurs without any moving parts or environmental emissions during operation. It is well proven, as photovoltaic systems have now been used for fifty years in specialized applications, and grid-connected PV systems have been in use for over twenty years.[2]

Driven by advances in technology and increases in manufacturing scale and sophistication, the cost of photovoltaics has declined steadily since the first solar cells were manufactured,[2][3] and the levelised cost of electricity (LCOE) from PV is competitive with conventional electricity sources in an expanding list of geographic regions.[4] Net metering and financial incentives, such as preferential feed-in tariffs for solar-generated electricity, have supported solar PV installations in many countries.[5] With current technology, photovoltaics recoup the energy needed to manufacture them in 1.5 (in Southern Europe) to 2.5 years (in Northern Europe).[6]

Solar PV is now, after hydro and wind power, the third most important renewable energy source in terms of globally installed capacity. More than 100 countries use solar PV. Installations may be ground-mounted (and sometimes integrated with farming and grazing) or built into the roof or walls of a building (either building-integrated photovoltaics or simply rooftop).

In 2013, the fast-growing capacity of worldwide installed solar PV increased by 38 percent to 139 gigawatts (GW). This is sufficient to generate at least 160 terawatt hours (TWh) or about 0.85 percent of the electricity demand on the planet. China, followed by Japan and the United States, is now the fastest growing market, while Germany remains the world's largest producer, contributing almost 6 percent to its national electricity demands.[7][8][9]

Photovoltaics are best known as a method for generating electric power by using solar cells to convert energy from the sun into a flow of electrons. The photovoltaic effect refers to photons of light exciting electrons into a higher state of energy, allowing them to act as charge carriers for an electric current. The photovoltaic effect was first observed by Alexandre-Edmond Becquerel in 1839.[11][12] The term photovoltaic denotes the unbiased operating mode of a photodiode in which current through the device is entirely due to the transduced light energy. Virtually all photovoltaic devices are some type of photodiode.

Solar cells produce direct current electricity from sun light which can be used to power equipment or to recharge a battery. The first practical application of photovoltaics was to power orbiting satellites and other spacecraft, but today the majority of photovoltaic modules are used for grid connected power generation. In this case an inverter is required to convert the DC to AC. There is a smaller market for off-grid power for remote dwellings, boats, recreational vehicles, electric cars, roadside emergency telephones, remote sensing, and cathodic protection of pipelines.

Photovoltaic power generation employs solar panels composed of a number of solar cells containing a photovoltaic material. Materials presently used for photovoltaics include monocrystalline silicon, polycrystalline silicon, amorphous silicon, cadmium telluride, and copper indium gallium selenide/sulfide.[13] Copper solar cables connect modules (module cable), arrays (array cable), and sub-fields. Because of the growing demand for renewable energy sources, the manufacturing of solar cells and photovoltaic arrays has advanced considerably in recent years.[14][15][16]

Solar photovoltaics power generation has long been seen as a clean energy technology which draws upon the planet’s most plentiful and widely distributed renewable energy source – the sun. The technology is “inherently elegant” in that the direct conversion of sunlight to electricity occurs without any moving parts or environmental emissions during operation. It is well proven, as photovoltaic systems have now been used for fifty years in specialised applications, and grid-connected systems have been in use for over twenty years.

Cells require protection from the environment and are usually packaged tightly behind a glass sheet. When more power is required than a single cell can deliver, cells are electrically connected together to form photovoltaic modules, or solar panels. A single module is enough to power an emergency telephone, but for a house or a power plant the modules must be arranged in multiples as arrays.

Photovoltaic power capacity is measured as maximum power output under standardized test conditions (STC) in "Wp" (Watts peak).[17] The actual power output at a particular point in time may be less than or greater than this standardized, or "rated," value, depending on geographical location, time of day, weather conditions, and other factors.[18] Solar photovoltaic array capacity factors are typically under 25%, which is lower than many other industrial sources of electricity.[19]

Current developments

For best performance, terrestrial PV systems aim to maximize the time they face the sun. Solar trackers achieve this by moving PV panels to follow the sun. The increase can be by as much as 20% in winter and by as much as 50% in summer. Static mounted systems can be optimized by analysis of the sun path. Panels are often set to latitude tilt, an angle equal to the latitude, but performance can be improved by adjusting the angle for summer or winter. Generally, as with other semiconductor devices, temperatures above room temperature reduce the performance of photovoltaics.[20]

A number of solar panels may also be mounted vertically above each other in a tower, if the zenith distance of the Sun is greater than zero, and the tower can be turned horizontally as a whole and each panels additionally around a horizontal axis. In such a tower the panels can follow the Sun exactly. Such a device may be described as a ladder mounted on a turnable disk. Each step of that ladder is the middle axis of a rectangular solar panel. In case the zenith distance of the Sun reaches zero, the "ladder" may be rotated to the north or the south to avoid a solar panel producing a shadow on a lower solar panel. Instead of an exactly vertical tower one can choose a tower with an axis directed to the polar star, meaning that it is parallel to the rotation axis of the Earth. In this case the angle between the axis and the Sun is always larger than 66 degrees. During a day it is only necessary to turn the panels around this axis to follow the Sun. Installations may be ground-mounted (and sometimes integrated with farming and grazing)[21] or built into the roof or walls of a building (building-integrated photovoltaics).

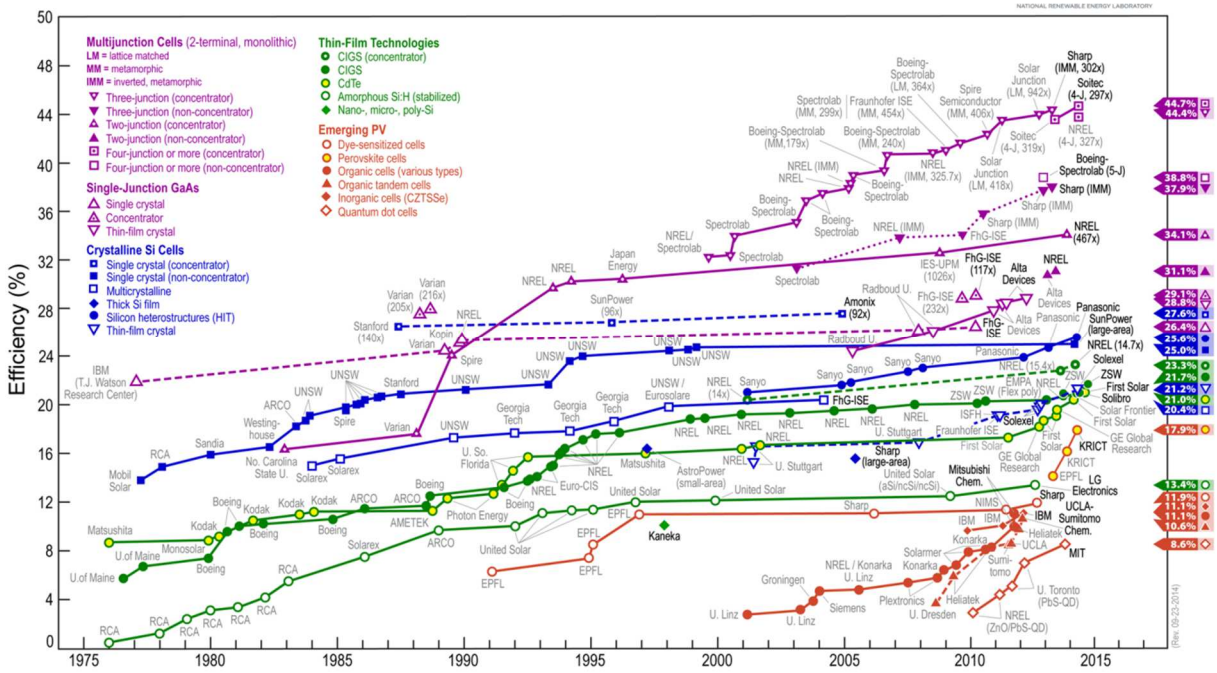

Fig. 10. Best Research-Cell Efficiencies

The San Jose-based company Sunpower produces cells that have an energy conversion ratio of 19.5%, well above the market average of 12–18%.[22] The most efficient solar cell so far is a multi-junction concentrator solar cell with an efficiency of 43.5%[23] produced by Solar Junction in April 2011. The highest efficiencies achieved without concentration include Sharp Corporation at 35.8% using a proprietary triple-junction manufacturing technology in 2009,[24] and Boeing Spectrolab (40.7% also using a triple-layer design).

Several companies have begun embedding power optimizers into PV modules called "smart modules". These modules perform maximum power point tracking (MPPT) for each module individually, measure performance data for monitoring, and provide additional safety. Such modules can also compensate for shading effects, wherein a shadow falling across a section of a module causes the electrical output of one or more strings of cells in the module to fall to zero, but not having the output of the entire module fall to zero.[25]

Solar photovoltaics is growing rapidly, albeit from a small base, to a total global capacity of 139 gigawatts (GW) at the end of 2013. The total power output of the world's PV capacity in a calendar year is equal to some 160 billion kWh of electricity.[8][27] This is sufficient to cover the annual power supply needs of 40 million households in the world, and represents 0.85 percent of worldwide electricity demand. More than 100 countries use solar PV.[9][28] China, followed by Japan and the United States is now the fastest growing market, while Germany remains the world's largest producer, contributing almost 6 percent to its national electricity demands.[7] Photovoltaics is now, after hydro and wind power, the third most important renewable energy source in terms of globally installed capacity.[29]

The 2014 European Photovoltaic Industry Association (EPIA) report estimates global PV installations to grow 35-52 GW in 2014. China is predicted to take the lead from Germany and to become the world's largest producer of PV power in 2016. By 2018 the worldwide photovoltaic capacity is projected to have doubled (low scenario of 320 GW) or even tripled (high scenario of 430 GW) within five years. The EPIA also estimates that photovoltaics will meet 10 to 15 percent of Europe's energy demand in 2030.

The EPIA/Greenpeace Solar Generation Paradigm Shift Scenario (formerly called Advanced Scenario) from 2010 shows that by the year 2030, 1,845 GW of PV systems could be generating approximately 2,646 TWh/year of electricity around the world. Combined with energy use efficiency improvements, this would represent the electricity needs of more than 9 percent of the world's population. By 2050, over 20 percent of all electricity could be provided by photovoltaics.[30]

4.2. Main thin film technologies

4.2.a. *a-Si/c-Si tandem cells, structure, production.*
4.2.b. *CIGS based cells, structure, production.*
4.2.c. *TCO (transparent conductive oxides) in solar cells*

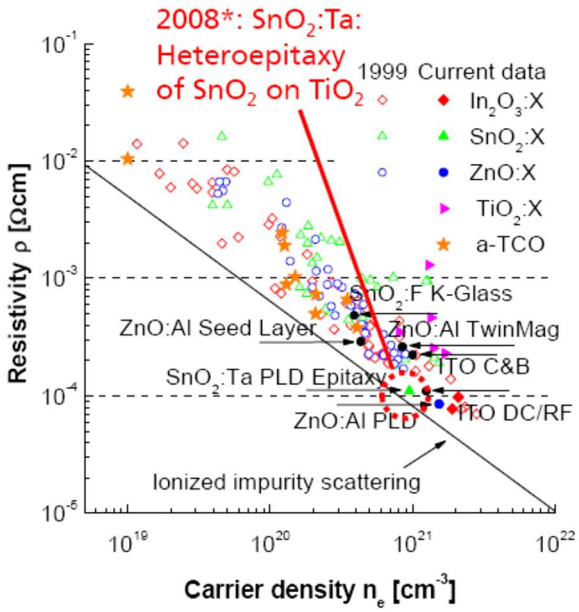

*Fig. 9. The classical view: r = f(n_e). [J. R. Bellingham et al., J. Mat. Sci. Let. 11 (1992) 263 | *: H. Toyosaki et al., APL 93 (2008) 132109].*

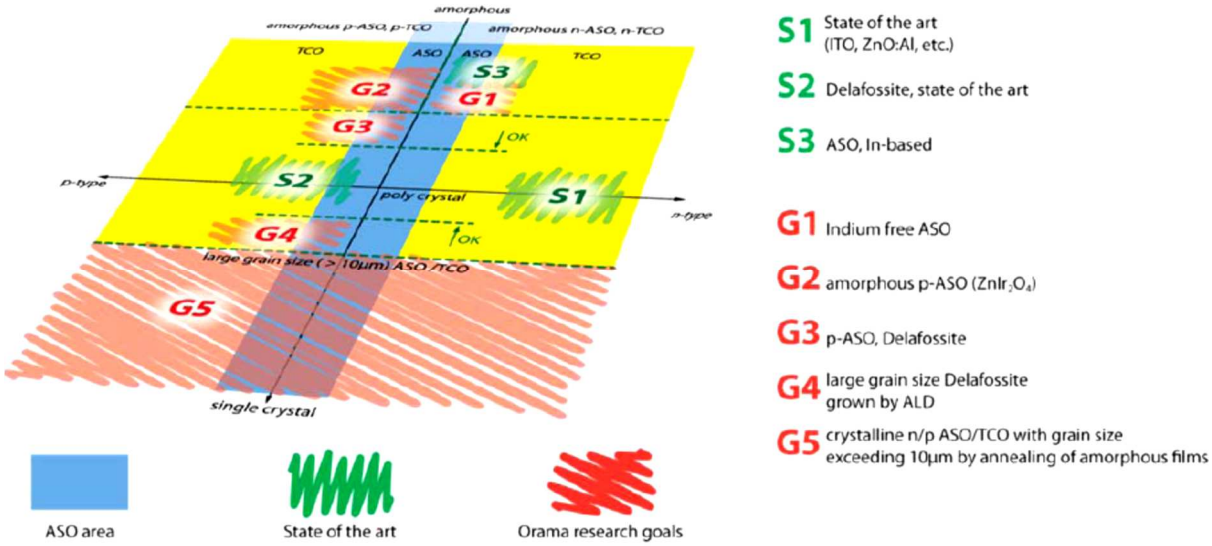

Fig. 10. New view: morphology vs. doping. "from p to n and from single crystal to amorphous"[Current Applied Physics – in press].

Two perspectives on TCOs:

- Optimization of doping mechanisms and minimization of free electron scattering.
- Limit: Ionized impurity scattering
- Indium based films reach the theoretical limit while need for improvement exists for other materials.
- New approaches:

- Suppression of dopant segregation
- Explosive crystallization (e. g. SnO2:Ta and TiO2:Nb)
- Amorphous TCOs

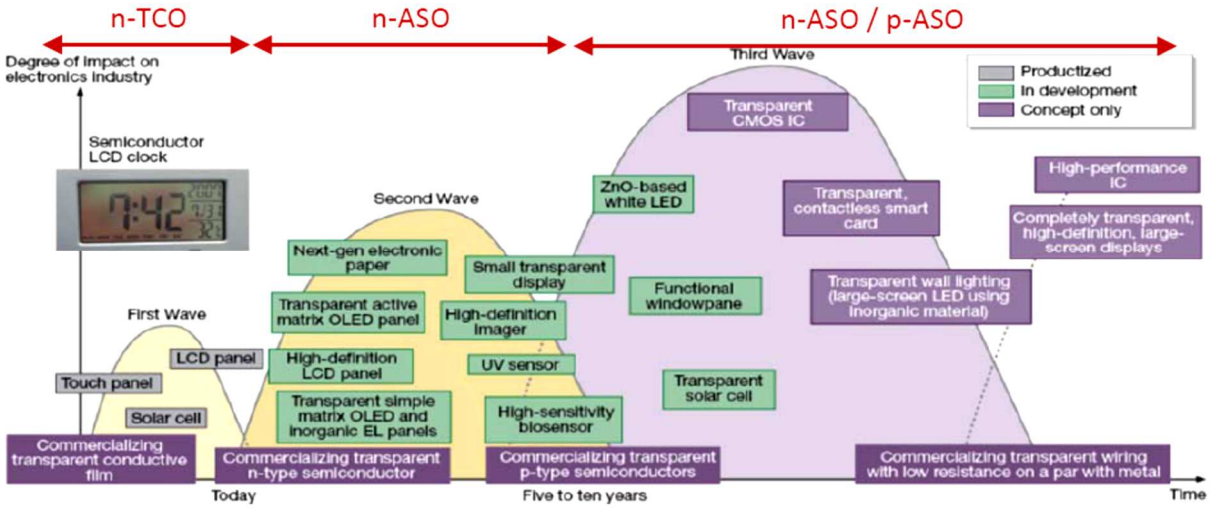

Fig. 10. Road map for oxide based, transparent electronics. [Nikkei Electronics Asia November 2007 – Transparent electronic products soon a reality].

1st wave: n-TCOs as transparent conductors
2nd wave: n-ASOs for oxide TFTs and related products
3rd wave: oxide p-n junctions for oxide LEDs and oxide μ-electronics

4.3. Characterization of efficiency (sun simulator, I-V curves, mapping).

5. New concepts and materials in energy saving technologies.

5.1. New concepts and materials in Photovoltaics (PV).

5.1.a. *Hybrid organometallic halide perovskite absorber based PV.*

5.1.b. *Dye-sensitized solar cells, organic PV.*

5.1.c. *New concepts of batteries.*

5.2. Oxide electronics: advantages, state-of-the-art.

Questions:
- Where do thin-film applications play a role
- Give examples for thin film deposition techniques and describe their principle
- Why are plasma techniques so important
- Difference between sputtering and PECVD
- Explain thin-film growth step by step
- Discuss: economic factors for industrial production of thin films

Under the same gas-phase supersaturation, cube-shaped nuclei are observed to form homogeneously in the gas and heterogeneously both on a flat surface and at right-angle steps on this surface. For each of these sites calculate the critical nucleus size and energy barrier for nucleation.
Film is deposited on a substrate by means of evaporation. In the expression for the rate of heterogeneous nucleation, identify which terms are primarily affected by:
raising the temperature of the evaporant source;
changing the substrate material;
doubling the source-substrate distance;
raising the substrate temperature;
improving the system vacuum;
In each case qualitatively describe the nature of the change.

During examination of the grain structure of a film evaporated from a point source onto a large planar substrate, the following observations were made as a function of position:
there is a film thickness variation;
there is a grain size variation;
there is a variation in the angular tilt of columnar grains.
Explain the physical reasons for these observations.